NASA CR-111859

THE PERKIN-ELMER CORPORATION
AEROSPACE DIVISION
2855 Metropolitan Place, Pomona, California 91767

FINAL REPORT
DIRECT ENTRY ACCUMULATOR CELL-MOLECULAR BEAM ION SOURCE
VOLUME 5 OF 6
FOR
COMBINED STUDY PROGRAM

By Mary Rotheram
and
M.R. Stevens

March 1971

Contract NAS1-9469
SPO Number 30006

Prepared for

NATIONAL AERONAUTICS AND SPACE ADMINISTRATION
LANGLEY RESEARCH CENTER

Langley Station
Hampton, Virginia 23365

NASA CR-111859

THE PERKIN-ELMER CORPORATION
AEROSPACE DIVISION
2855 Metropolitan Place, Pomona, California 91767

FINAL REPORT
DIRECT ENTRY ACCUMULATOR CELL-MOLECULAR BEAM ION SOURCE
VOLUME 5 OF 6
FOR
COMBINED STUDY PROGRAM

By Mary Rotheram
and
M.R. Stevens

March 1971

Approved By: M. Rotheram by MER Date 3/30/71
M. Rotheram, Senior Chemist

Approved By: M.R. Stevens by MER Date 3/30/71
M.R. Stevens, Project Engineer

Approved By: B.F. Bicksler Date 3/30/71
B.F. Bicksler, Project Manager

Approved By: M.R. Ruecker Date 30 March '71
M.R. Ruecker, Manager Space Physics

Approved By: W.C. Qua Date 30 Mar 71
W.C. Qua, Program Manager

Contract NAS1-9469
SPO Number 30006

Prepared for
NATIONAL AERONAUTICS AND SPACE ADMINISTRATION
LANGLEY RESEARCH CENTER
Langley Station
Hampton, Virginia 23365

ABSTRACT

A program was conducted in which an instrument system concept was studied to optimize the application of a mass spectrometer as a sensor for monitoring the primary atmospheric constituents, as well as atmospheric contaminants, on board a manned spacecraft. The program was divided into six individual studies representing the primary system parts complementing the spectrometer: A Carbon Monoxide Accumulator Cell (Volume 1), an Ion Pump (Volume 2), an Ion Pump Power Supply (Volume 3), an Inlet Leak (Volume 4), an Ion Source (Volume 5), and an Undersea Atmospheric Analyzer (Volume 6). The principle goal of the combined study program was the achievement of an instrument concept of minimum power, weight and size without compromising the minimum detection limits of the instrument.

TABLE OF CONTENTS

LIST OF ILLUSTRATIONS

MOLECULAR BEAM ION SOURCE

SUMMARY

The concept of a molecular beam ion source has a modest theoretical advantange over the conventional differentially pumped type. It may also have an advantage in terms of stability since surfaces bombarded by charged particles can be maintained in a relatively low pressure environment. While the degree of collimation of the molecular beam is substantial, in terms of the maximum beam axis, the solid angles are small near this point so that the actual flux is not as well collimated as it would first appear. Therefore, in order to achieve a high molecular density at the point of ionization, it will be necessary to place the electron beam as close as possible to the molecular beam entrance point. This will require careful design and possibly the use of a magnetically confined electron beam. The physical requirements of the direct entry ion source, in particular the array of sample inlet tubes, appear to be feasible and the pressures involved in the inlet system ahead of the sample inlet tubes are compatible with accumulator cell operation.

Principles involved in the design of an inlet system for trace contaminant analysis with the accumulator cell concept were reviewed. Design of a system that does not require a bypass pumping line was shown to be feasible if some means can be provided for reducing the cell pressure from atmospheric to about two-tenths of a torr. System performance was considered and it appears that sensitivity comparable to that obtained in the Laboratory Contaminant Sensor System, one-tenth to ten parts per million, could be realized.

Original system considerations were based on the use of linear temperature programmed desorption. It appears feasible, on the basis of results obtained in the Carbon Monoxide Accumulator Cell Program, to use stepped temperature programming with a resultant increase in sensitivity. However, use of this mode of operation is restricted to analysis of relatively simple contaminant mixtures since it does result in loss of some of the separation afforded by linear temperature programming.

INTRODUCTION

The feasibility of detecting and determining a wide range of trace contaminants in air by an adsorption preconcentration technique was demonstrated in the development of a Laboratory Contaminant Sensor under

NASA/Langley Research Center Contract NAS1-7266. An extension of this effort, under NAS1-8258, lead to increased sensitivity of the instrument permitting detection of contaminants at concentrations of less than one part per million and investigated the instrument performance with a much wider range of concentration.

Since the primary objective of these efforts was to develop an instrument capable of performing contaminant analysis on board a manned spacecraft, it is essential that the optimization of the instrument, to achieve minimum power, weight and size, be kept as one of the primary goals. At the same time the detectable limit for the instrument cannot be compromised. This study is concerned with the analysis of a design concept which appears to offer an advantage in this area by making the maximum utilization of the available sample. This is accomplished by a twofold process. The first part of the process involves the direct entry of sample from the accumulator cell into the ion source and the second the direction of the entering sample gas into a molecular beam in order to increase the sample density in the ion source and achieve enhanced sensitivity.

GENERAL DISCUSSION

In the Laboratory Contaminant Sensor, after a sample has been concentrated in the accumulator cell, the analysis is performed by heating the cell to desorb the contaminant into the inlet system of the mass spectrometer. The mass spectral signal depends on the pressure of the contaminant in the inlet system at any given time. This is in turn controlled by the rate at which the cell is heated to desorb the contaminants and the rate at which material is pumped out of the system through the bypass valve. Relatively large samples are employed, but only a small fraction of the total contaminant sample enters the mass spectrometer ion source through the gold leak; the remainder is pumped away through a bypass valve. This is basically an inefficient use of the contaminant sample. Much smaller air samples could be used if all of the accumulated contaminants could be introduced into the ion source. This would eliminate the bypass line pump and reduce the power requirements for the system. Some vacuum source is still needed to precut air from the cell, but the requirements for this source are much less stringent than those for continuous operation of the bypass line.

With small samples, the size of the inlet system and accumulator cell must be reduced so that the pressure in front of the gold leak and the ratio of the volume to conductance (time constant) remain approximately the same as the larger system. (This is not a tight requirement. There is a range of values for the pressure and time constant that will yield the

desired sensitivity and analysis time.) With a smaller inlet system and accumulator cell, the heating power consumed is less and the required capacity of the pump for the precut operation is also less.

Another factor to be considered is the design of the ion source to obtain the sensitivity required to detect the lowest concentration of contaminants of interest. The ion source sensitivity is related to the requirements of the analyzer with which it will be integrated and the available pumping speed for sample flow. An analysis of the tradeoffs, which are involved in going to higher ion source pressures under conditions of constant available pumping speed, was conducted under contract NAS5-3453. This analysis indicated that the higher the maximum ion source pressure allowed the greater the ion current output would be. These considerations will have a strong impact upon the design of the ion source but must be weighed against the likelihood of increased ion source contamination at higher pressures.

The design goals then are to obtain a high ion current yield, at a source pressure that is as high as possible, consistent with limitations imposed by space charge effects, analyzer pressure and formation rate of surface deposits.

If all the sample is to be pumped through the mass spectrometer there is an upper limit to the amount of sample that can be utilized. This is determined by the required analysis time period and the speed of the mass spectrometer pump. The flow rate through the vacuum system must be low enough that the pump can maintain the analyzer pressure at the required low pressure (10^{-6} torr, maximum).

$$Q = P_a S_p$$

Q = Flow rate (torr-cc/sec)

P_a = Analyzer pressure (torr)

S_p = Speed of the pump for contaminants at the analyzer pressure (cc/sec)

Assuming a desorption time period of twenty minutes for each sorbent cell, the maximum sample that can be accumulated is approximately the product of the flow rate and the heating time period. For example, if a pump speed of one liter per second is considered and a maximum analyzer pressure of 10^{-6} torr, the total sample allowed to enter the mass spectrometer cannot exceed 1200 torr microliter or one and six-tenths atmospheres microliter of total sample.

Assuming that an ion source with a differential pumping ratio of fifty is used, the source pressure would be 5×10^{-5} torr. To obtain this pressure with an inlet pressure of fifty microns and a flow of 10^{-6} torr-liters per second, the leak conductance must be 2×10^{-5} liters per second. A small orifice of about fourteen microns in diameter would be adequate. To maintain a constant comparable to that now used in the Laboratory Contaminant Sensor, a volume of about 0.26 cubic centimeter would be required in the inlet system. This volume is small for a practical system; however, there are some tradeoffs between inlet pressure and volume, and leak conductance and time constant that can be utilized to arrive at a practical size for the volume which will meet the constraints of available pumping speed and required sensitivity. These numbers indicate that the direct entry approach is indeed feasible.

ION SOURCES

In any mass spectrometer the region in which ionization occurs at as high a pressure as possible is desirable in order to obtain good sensitivity or high ion current densities. The upper pressure that can be tolerated is chiefly limited by ion space charge effects, although mean free path considerations can become important at higher pressures. The pressure in the mass analyzer is restricted to low values in order to minimize collision of the ion beam with background gas molecules. For electron impact ionization, the filament is also operated outside the source in order to minimize collection of ions produced by reaction of the sample gas with the filament and to give maximum filament life.

Normally, for flight instruments the analyzer and ion source are operated from the same vacuum pump, and therefore, the pressure in the ion source is established by the flow through the system and the conductance of the ion source. The source conductance is in turn determined by the size of the openings required for the electron beam entrance and exit and the ion beam exit. This is characteristic of the differentially pumped ion source. A schematic diagram of a typical differentially pumped ion source is shown below.

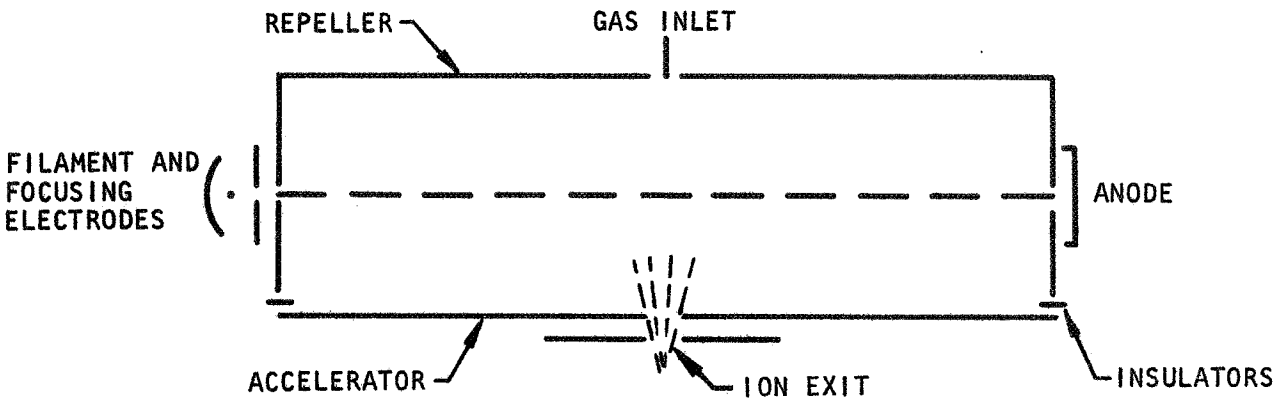

An alternate method of obtaining high gas densities in the ionization region is through the use of a molecular beam. By channeling the entering gas stream through a relatively long aperture, the molecules enter the ionization region primarily in the forward direction from the aperture. The gas density at the exit from the leak is high and decreases as the beam traverses the ionization region and spreads out into the chamber. By choosing the intersection of the electron beam with the molecular beam close to the exit aperture, obtaining the same ion current may be possible from this type of source as from the differentially pumped sources. A molecular beam ion source with open grid electrodes is shown below.

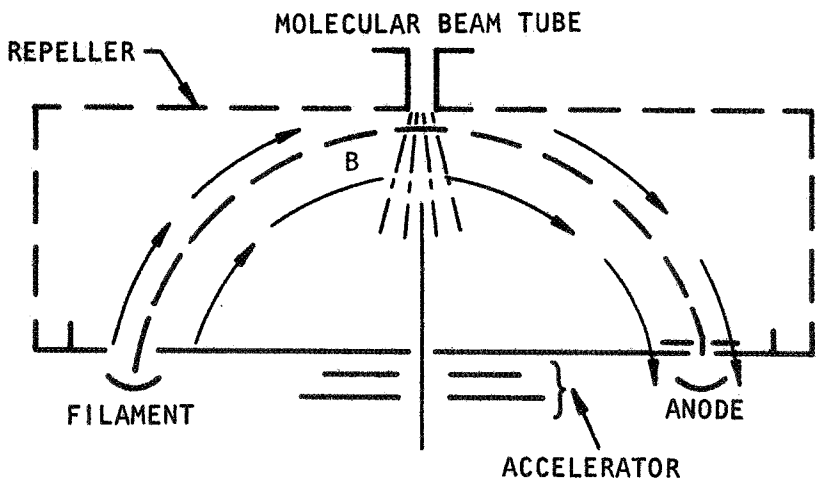

Both sources have problems unique to their design. In the differentially pumped source, the walls of the source are the electrodes, which control ion beam extraction and the electron beam path and are constantly exposed to materials that can cause surface deposits. These deposits are insulating in nature and the buildup of surface charges due to impacts of ions and electrons result in field distortion in the ion source and loss of sensitivity. The formation rate of deposits can be controlled to a certain extent by increasing the temperature of the source. Mass spectral patterns are affected by the ion source temperature, however, and an optimum operational temperature will exist which will minimize contamination.

The molecular beam source on the other hand can be a relatively open source. The electrode surface area can be minimized and the pressure outside the beam may be relatively low. The sensitivity however will depend on the gas density, which can be obtained in the beam, and since the beam intensity decreases as the square of the distance from the leak, it will be necessary to bring the electron beam through the molecular beam fairly close to the exit aperture. The ions will be formed in a relatively small area, which should lead to good collection efficiency. This source will require a high degree of control in the position of the electron beam, which implies that a constraining magnetic field be employed. The advantage of this source is the fact that the same molecular density may be achieved in a narrow beam with a lower flow through the system than for a differentially pumped source, or conversely, for the same flow, a more intense ion beam or an increase in sensitivity can be achieved.

Filament interaction with the sample is an important factor in ion source design. Reactions of the sample with the hot filament can result in production of ion species which, if extracted into the ion beam, lead to erroneous sample analysis. Such reactions also shorten the filament lifetime. In differentially pumped ion sources, the filament is usually located outside the source in a region of pressure intermediate between that of the source and the analyzer. This will also be true for a molecular beam source. The filament itself is usually shielded in such a way that reaction products will not enter the source or be extracted as part of the ion beam. However, such reactions will still decrease the lifetime of the filament and are therefore a factor in establishing the upper pressure limit for the source. The reaction rate depends on the filament operation temperature and will be faster at higher temperatures. Since the electron beam current depends in part on the filament temperature and determines the ion current yield, the tradeoffs between filament lifetime and source sensitivity must be examined carefully for any ion source.

MOLECULAR BEAM DIRECT ENTRY ION SOURCE

Basically, the parameters that define the ion current producing capabilities of a given ion source are, first, the electron current density, second, the electron path length, third, the ionization cross section of the gas molecules, and fourth, the gas density. For an ion source of a given geometry, the first three parameters become invariant under normal operating conditions. Only the gas density is variable, with the ion current produced being proportional to the gas density in the vicinity of the electron beam.

Practical considerations limit the gas density within the ion source. Source pressures on the order of 10^{-4} to 10^{-6} torr are optimum for successful long term source operation. At higher source pressures, filament life is reduced, ion to molecule and molecule to molecule interactions take place and formations will be deposited on the electrodes. With reactive gases, ion to molecule interactions as well as molecule to molecule interactions may well invalidate the mass spectral data. This is particularly true with respect to the Laboratory Trace Contaminant Sensor System where the concentrated gases monitored are largely composed of reactive gases. An increase in the number of gas molecules interacting with the electron beam is invariably accompanied by an increase in the pumping requirements of the differentially pumped source in order to maintain the above cited overall source pressures.

On the other hand, achieving higher gas densities in the vicinity of the electron beam is possible without increasing the total flow of gas through the source, therefore, without increasing the pumping requirements of the system. Such an arrangement may be attained by utilizing directed low pressure gaseous beams and is directly applicable to the Laboratory Trace Contaminant Study.

The purpose of this section is to establish the requirements for a directed gas beam entry ion source. Results of the analysis detailed below show that this type of source is feasible.

Formation of Directed Gas Beam

Gaseous beams of the type considered here are best achieved under molecular flow conditions, i.e., at pressures expressed by the following inequality,

$$P < \frac{15 \times 10^{-3}}{a} \qquad (1)$$

where P = Pressure torr

a = Characteristic dimension of orifice through which gas is flowing (cm).

For the ideal orifice, a, is the radius of the orifice and

$$a >> L \tag{2}$$

where L is the length of the orifice. At pressures defined by Equation (1), the mean free path, λ, of the gas is related to the orifice radius and length by the inequality

$$\lambda >> a >> L \tag{3}$$

In practice, achieving an ideal orifice is impossible. Instead, orifices are employed wherein $L \geq a$. For such orifices, λ may assume one of the following inequalities,

$$\lambda >> L \geq a \tag{4}$$

$$\lambda \leq L > a \tag{5}$$

$$\left.\begin{array}{l} L > L_o > Z_o \\ \lambda > L < L_o > a \end{array}\right\} \tag{6}$$

$$\left.\begin{array}{l} L > Z_o > L_o \\ \lambda < L > Z_o > L_o >> a \end{array}\right\} \tag{7}$$

In the above equations, L_o is the distance near the discharge end of the orifice where Knudson flow is present and Z_o is a distance from the discharge end of the orifice.

For an infinitely small orifice, the number of molecules effusing out of the orifice is given by:

$$I_t = A\nu \tag{8}$$

where A = Cross sectional area of the orifice

ν = Number of molecules effusing from an orifice of unit area per second.

For a nonideal orifice, one that is not infinitely small, Equation (8) is still applicable when modified by a factor T, taking the form,

$$I_t = TA\nu \tag{9}$$

The factor, T, is always less than unity and is a function of the geometry of the system. Nonideal orifices are generally cylindrical, rectangular or conical in shape. Since the present effort is centered about gas beams effusing from long cylindrical tubes, the factor is expressed as,

$$T = 8/3\ (a/L) \tag{10}$$

and indicates the extent to which the flow out of the orifice is attenuated by the geometry of the orifice. In Equation (10) (a) and (L) retain their previous definitions. The fact that the total flow out of a nonideal orifice is always less than the total flow from an ideal orifice proves advantageous in developing the directed gas beam source. This is particularly true when considering the angular distribution of the effusing molecules and their number density relative to the total flow from the orifice.

A molecule on the upstream side of an ideal orifice will not necessarily be in a position such that it will travel toward the opening in a direction normal to the opening. As shown by Figure 1, the molecule may travel toward the opening at an angle Θ, with normal and will leave the orifice at an angle Θ, relative to the downstream normal, within a solid angle $d\omega$. The number of molecules that emerge from the orifice within the solid angle, $d\omega$, is proportional to the area of the orifice normal to their direction, A cos Θ, the number that strikes a unit surface per second, I/A, and the ratio of the solid angle, $d\omega$, to the total solid angle available to all the emerging molecules, $d\omega/2\Pi$. This is expressed as:

$$I(\Theta) = \kappa I \cos\Theta \frac{d\omega}{2\Pi} \tag{11}$$

where κ is the proportionality constant. The value of κ is determined by setting $d\omega = 2\Pi \sin\theta \, d\theta$ and integrating the equation between the limits of 0 to $\Pi/2$,

$$\int_0^{\Pi/2} I(\theta) d\omega = \int_0^{\Pi/2} \frac{\kappa I \, 2\Pi \sin\theta \cos\theta \, d\theta}{2\Pi} \tag{12}$$

and since

$$\int_0^{\Pi/2} I(\theta) \, d\omega = I \tag{13}$$

$\kappa = 2$. Equation (11) becomes,

$$I(\theta) = I \cos\theta \frac{d\omega}{\Pi} \tag{14}$$

and applying Equation (8) for the value of I we have,

$$I(\theta) = A\nu \cos\theta \frac{d\omega}{\Pi} \tag{15}$$

Clausing[1] determined the distribution $I(\theta)$ for an ideal orifice and for the case of a short tube of $L/a = 2$. These data may be found in several texts[2,3] based upon Equation (15), for the ideal orifice, and,

$$I(\theta) = T' A\nu \cos\theta \frac{d\omega}{\Pi} \tag{16}$$

for the tube. In Equation (16), $T' \neq T$, the geometric factor of Equation (10). T' is a complicated function of tube geometry and Θ, and has values that decrease as θ increases.

Examination of Clausings data[1] shows that the number of molecules effusing out of the tubular orifice at values of θ of zero to ten degrees, with respect to the normal, is as great as obtained utilizing an ideal orifice. At the same time, fewer molecules leave the tube orifice at angles θ greater than ten degrees than from the ideal orifice. In addition, the total number of molecules emerging from the tube is approximately one-half the number leaving the ideal orifice.

The point here is that through the application of a tube, of relatively little departure from an ideal orifice, it is possible to achieve a gas beam of intensity virtually equal to that issuing from an ideal orifice flowing in the normal direction and a marked reduction in the total gas flow through the tube. Therefore, enhancing the flow in the normal direction should be possible by increasing the upstream pressure, or by using a number of tubes. This may be accomplished without increasing the pumping requirements of the system.

Direct application of Clausing's data could not be carried out. His method of evaluation necessitates reviewing the original articles, which were not available. Further, rather practical considerations indicate that the evaluation of tubes of different L/a ratios (>> 2) should be made under conditions where Equations (5) through (7) are applicable and not at $\lambda >> L$ as Clausing did. While optimum beam formation is achieved under 100 percent collision free parameters, the beam molecular density is very low. The attainment of relatively dense gas beams indicate the utilization of nonideal flow conditions, i.e., $\lambda = L$ or pressures higher than that expressed by Equation (1).

This approach to the problem is similar to that taken by Giordmaine and Wang[6]. The effusing beam is considered as a function of source geometry, angular distribution and the number of molecules that do (or do not) have collision upstream of the orifice prior to emerging from the tube. In effect, this approach permits one to extend the scope of Equation (16) to semiopaque sources, having values of $L/a >> 2$, over pressure ranges in excess of Equation (1).

Assume a cylindrical tube length of L, and radius, a, such that $L >> a$. At a distance, z, from the low pressure end of the tube consider a volume element within the tube equal to $\pi a^2 dz$. Let X be the number of collisions the molecules experience per second per unit volume of the tube. Then,

$$Y = X\ (\pi a^2 dz) \tag{17}$$

the number of collisions within the volume element under consideration. Since,

$$X = 2n^2\sigma^2 \left[\frac{\pi RT}{m}\right]^{1/2} \tag{18}$$

Equation (17) becomes,

$$Y = 2n^2\sigma^2\left[\frac{\Pi RT}{m}\right]^{1/2} \Pi a^2 dz \tag{19}$$

$$\frac{Y = n^2\sigma^2\Pi^2 a^2 \bar{c} dz}{\sqrt{2}} \tag{20}$$

after making the substitution

$$\bar{c} = 2\left[\frac{2RT}{\Pi m}\right]^{1/2}$$

In Equations (19) and (20),

n = Molecules/cm^3

σ = Molecular diameter, cm

$\bar{c}$ = Average molecular velocity in tube, cm/sec

m = Molecular weight

As a result of these collisions, there will be a number of molecules leaving the volume element in the direction of the tube axis and effusing from the tube within the solid angle, $d\omega$, which is $d\omega/2\Pi$ of the total solid angle embracing all of the emerging molecules. This number of molecules is, β, where,

$$\beta = Y\frac{d\omega}{2\Pi} \tag{21}$$

or

$$\beta = \frac{n^2\sigma^2\Pi a^2\bar{c}dzd\omega}{2\sqrt{2}} \tag{22}$$

Of the β molecules, given by Equation (22), a certain number will not undergo further collisions. Assuming the molecules are travelling at u centimeters per second and that a molecule may have A collisions per second, then A/u = collisions per centimeter per molecule. In the distance dz, a

molecule makes A/u dz collisions. For the β molecules at hand, the total number of collisions is β (A/u)dz. This represents the decrease in β, i.e., -2 dβ, since each collision involves two molecules. Hence,

$$\beta\ (A/u)dz = -2\ d\beta \tag{23}$$

and

$$\beta_o \exp\ [-1/2\ (A/u)Z] \tag{24}$$

But $A/u = 1/\lambda$, therefore,

$$\beta_o \exp\left[-\frac{\Pi\sigma^2 r z^2}{\sqrt{2}}\right] \tag{25}$$

the number of molecules that emerge from the tube without a further collision. In Equation (25), the following substitutions were made,

$$\lambda = 1/\left(\sqrt{2}\ n\Pi\sigma\right)$$

$$n = rz$$

where r is a constant determined by the flow rate of the molecules in the tube

λ = Mean free path

and β_o is the number of molecules originally present and is equal to the value of β in Equation (22).

Consequently, the total number of molecules that emerge from the orifice in the direction of the tube axis, within the solid angle, dω, is I(0,z) dωdz where,

$$I(0,z)d\omega dz = \frac{\Pi a^2\sigma^2 r^2 z^2 \bar{c}}{2\sqrt{2}}\ \exp -\left[\frac{\Pi\sigma^2 r z^2}{\sqrt{2}}\right] d\omega dz \tag{26}$$

Integration of Equation (26) yields the total contribution to I(0) arising from collisions throughout the tube. Then

$$\int_o^{z=L} I(0,z)d\omega dz = I(0)d\omega \tag{27}$$

and

$$I(0)\,d\omega = \frac{\Pi a^2 \sigma^2 r \bar{c} d\omega}{2\sqrt{2}} \int_o^L \exp -\left[\frac{\Pi \sigma^2 r z^2}{2}\right] z^2 dz \qquad (28)$$

which becomes,

$$I(0)\,d\omega = \frac{a^2 \bar{c} r^{1/2} d\omega}{\Pi^{1/2} \sigma\, 2^{7/4}} \int_o^{L'} \exp\left[-y^2\right] dy - \frac{\bar{c} a^2 r L d\omega}{4}\ \beta^{-(L')^2} \qquad (29)$$

After setting

$$y = \left(\frac{\Pi \sigma^2 r}{\sqrt{2}}\right)^{1/2} z \text{ and } L' = \left(\frac{\Pi \sigma^2 r}{\sqrt{2}}\right)^{1/2} L$$

all other terms being previously defined.

The only other contribution to I(0) arises from those molecules that pass through the entire tube without a collision. By an analysis similar to that cited above, this number of molecules is

$$\frac{c\, r\, a^2 L\, d\omega}{4}\ \varepsilon^{-(L')^2}$$

Summing this value and Equation (29) yields the total contribution to I(0);

$$I(0) = \frac{3^{1/2}\, c^{1/2}\, a^{1/2}\, n^{1/2}}{4 \cdot 2^{1/4}\, \Pi \sigma} \int_o^{L'} \exp(-y^2) dy \qquad (30)$$

after substituting

$$r = 3n/(2\Pi c a^3)$$

$$L' = \frac{3^{1/2}\, \sigma\, L\, n^{1/2}}{2^{3/4}\, c^{1/2}\, a^{3/2}}$$

where n equals the flow rate through the tube (molecules/sec). Equation (30) expresses I(0) in units of molecules per steradian per second. I(0) is the peak intensity of the emergent beam in the direction of the tube axis, i.e., at $\theta = 0$.

The beam intensity at angles other than $\theta = 0$, is evaluated in an analogous manner. Because of the rather lengthy development involved, only the equation for the integrated beam intensity [$I(\theta)$] is presented and is,

$$I(\theta) = \frac{3^{1/2}\, a^{1/2}\, c^{1/2}\, n^{1/2}}{2^{1/4}\, \Pi^2 \sigma} (\cos^{3/2}\theta) \int_0^1 \int_0^{kz'} [1 - (z')^2]^{\frac{1}{2}} \exp(-y^2) dy dz \tag{31}$$

where $z' = \frac{z \tan\theta}{2a}$ and $\kappa = \left(\frac{\Pi\sigma^2 r}{2\cos\theta}\right)^{1/2} \frac{2a}{\tan\theta}$

and all other terms being as previously defined.

Equations (30) and (31) permit the evaluation of the beam shape, in terms of the relative intensity, as a function of θ, L, a, and P, the upstream pressure. Applications of these equations are presented in the Development of Ion Source Parameters section of this report.

Development of Ion Source Parameters

Within the constraints of space charge limitations the most efficient ion source, in terms of ionizing efficiency, is one that allows the greatest number of gaseous molecules to interact with the ionizing electron beam. In the present case, this is to be accomplished without the necessity of large pumping requirements to maintain the required minimum overall pressure level in the ion source. Since the amount of gas flow into the system, $Q_{(in)}$ (torr cm^3/sec), must equal the gas flow out of the system i.e., the flow through the pump, $Q_{(out)}$, this equality for a directed beam type source is

$$Q_{in} = P_B V_B A_B = Q_{out} = P_{BK} S_P \left(\frac{\text{torr cm}^3}{\text{sec}}\right) \tag{32}$$

where S_P = Speed of the pump, cm^3/sec

P_{BKGD} = Background (BKGD) pressure = pressure at pump entrance, torr

A_B = Cross sectional area of gas beam, cm^2

V_B = Velocity of gas molecules, cm/sec

P_B = Beam pressure, torr

From Equation (32), it is evident that optimum operating conditions are achieved when the ratio P_B/P_{BKGD} is maximum, i.e.,

$$P_B/P_{BKGD} = \frac{S_P}{V_B A_B} = \text{maximum} \tag{33}$$

For a pump of a given S_P value and with V_B determined by the temperature of the beam and molecular weight of the gas in the beam, maximization of the ratio can only be achieved by minimizing the area of the beam, A_B. The problem is to achieve such an effect and at the same time maintain a relatively dense concentration of gaseous molecules in the vicinity of the electron beam. An individual molecular beam of the type described by Equations (30) and (31) will lead to beams having the desired value of A_B but of low values for P_B. However, by employing an array of such beams, the number density of the gaseous molecules will be increased significantly without appreciably distorting the value of the overall A_B from that of an individual beam. In fact, to a first approximation, only the background pressure requirements limit the number of beams within such an array. As will be shown an array of 100 beams is practical for this particular purpose.

Table 1 presents a synopsis of the typical data, pertinent to molecular beam characteristics, obtained during the course of this analysis. Data from the fourth column of Table 1, i.e., for tubes of one centimeter in length and P equal to five-tenths of a torr will be utilized to illustrate how these values were obtained. The first step in the analysis is to determine the beam intensity as a function of Θ. For this purpose Equations (30) and (31) are employed with the following parameters,

L = 1 cm; tube length

a = 1.7×10^{-3} cm, tube radius

M = 28, molecular weight of nitrogen, the gas assumed in this example

TABLE 1.- Computed Directed Gas Beam Ion Source
Data - N_2 Gas Assumed Throughout

P_g Torr	L cm	a cm x 10^{-3}	$\frac{L}{a}$	No. of Ducts	θ EFF Degrees	Molecules per Sec	h_B cm	V_B cm^3 x 10^{-5}	A_B cm^2 x 10^{-3}	$\frac{P_B}{P_{BK}}$	P_B torr x 10^{-5}	P_{BKG} torr x 10^{-6}	J+ A/cm^2 x 10^{-8}	Remarks
0.75	0.31	1.7	182	10	40	2.8×10^{14}	0.025	8	3.2	26	5.7	2.2	18	74% of beam within
				100	40	2.8×10^{15}					57.0	22.0	180	40° angle:
0.5	0.31	1.7	182	10	40	1.9×10^{14}	0.025	8	3.2	26	3.9	1.5	12	75% of beam within
				100	40	1.9×10^{15}					39.0	15.0	123	40° angle
	0.62	1.7	364	10	40	9.5×10^{13}	0.025	8	3.2	26	2	.75	6	
				100	40	9.5×10^{14}					20	7.6	62	
	1.00	1.7	588	10	35	5.6×10^{13}	0.025	5.5	2.2	38	1.7	0.4	4.5	72% of beam within
				100	35	5.6×10^{14}					17	4	45	35° angle
0.1	0.31	1.7	182	10	35	1.7×10^{13}	0.025	5.5	2.2	38	.50	0.13	1.3	70% of beam within
				100	35	1.7×10^{14}					5	1.3	13	35° angle

T = 300°K, absolute temperature

σ = 3.5×10^{-8} cm, molecular diameter

$\bar{c}$ = 4.76×10^{4} cm/sec, average velocity of gas molecules in the tube, evaluated from $\bar{c} = 14551\ (T/M)^{1/2}$

N = 7.82×10^{12} molecules/sec rate of flow of gas in the tube, evaluated from

$$N = (2/3)\ (\Pi)\ n_o \bar{c} \left(\frac{a^3}{L}\right)$$

n_o = Molecular density = 1.6×10^{16} molecules/cm^3 · torr evaluated from

$$\frac{10^{-3}}{m} \quad \frac{MP}{RT} = n_o$$

P_g = 0.5 torr, upstream gas pressure

m = 4.67×10^{-23} g/molecule, molecular mass for N_2.

Based upon these values, the constant term of Equation (30) becomes 83×10^{12} and,

$$I(0) = 83 \times 10^{12} \int_o^{L'} \varepsilon^{-y^2}\ dy \qquad (34)$$

The upper limit of integration in Equation (34) is given by the value of L' (see Equation (30)) and in this instance is 6.62. This value of L' indicates the source is opaque since the integral is virtually at its upper limting value, 0.886. Thus, the beam intensity in the forward direction is;

$$I(0) = 83 \times 10^{12}\ (0.886) = 7.35 \times 10^{13} \text{ molecules/ster/sec} \qquad (35)$$

The beam intensity as a function of Θ, where Θ is not equal to zero, is now evaluated using Equation (31). The double integral in this equation becomes k/3, and the first term has the value 105.7×10^{12} in this case. Then,

$$\frac{d}{\Theta} = I(\Theta) = 105.7 \times 10^{12} (\cos^{3/2} \Theta) (k/3) \tag{36}$$

where k is expressed as defined above. Using values of Θ zero to ten degrees is found to be:

$$I(2) = 23.1 \times 10^{12}$$

$$I(5) = 9.4 \times 10^{12}$$

$$I(10) = 4.5 \times 10^{12}$$

The beam shape, as defined by the relative intensities, is obtained by plotting the ratio $I(\Theta)/I(0)$ as a function of Θ. Figure 2 presents the beam shape so determined. As shown, approximately ninety percent of the beam intensity is contained within a five degree angular spread from the normal. The half-width angle of the beam $\Theta_{1/2}$, defined as the angle at which $I(\Theta) = \frac{I(0)}{2}$ is approximately one degree as shown.

Of greater importance however, is the molecular distribution of the beam. This distribution is evaluated by integrating Equation (31). Multiplication of Equation (31) by $d\omega$ leads to $I(\Theta)\, d\omega$ and,

$$I \text{ (molecules/sec)} = \int_{\theta_1}^{\theta_2} I(\theta)\, d\omega \tag{37}$$

Setting $d\omega = 2\Pi \sin \theta\, d\theta$, Equation (37) becomes,

$$I = 2\Pi \int_{\theta_1}^{\theta_2} I(\theta) \sin \theta\, d\theta \tag{38}$$

with $I(\Theta)$ equal to Equation (31). Integration of Equation (38) between the limits $\Theta_1 = 0$ and $\Theta_2 = \Pi/2$ leads to N/2, one-half the total number of molecules flowing from the tube. In this case the value obtained is 4.06×10^{12} molecules per second, which is in excellent agreement with the

value of N/2 as calculated from

$$N = (2/3)\ \Pi\ n_o c\ \frac{a^3}{L}\ ,$$

which is 3.91×10^{12} molecules per second.

Integration between other limits, i.e., $0 \rightarrow 2$, $2 \rightarrow 4$, etc., leads to the distribution curve shown in Figure 3. Based upon this curve, the integral Θ equals zero to Θ equals thirty-five degrees was selected for further evaluation of the source characteristics. Within that interval, approximately seventy-two percent of the beam molecules reside. The beam is in the form of a cone whose apex is at the tube orifice.

Assuming first that the electron beam could traverse the ionizing region 0.025 centimeters from the tube orifice, and second that the electron beam is in the form of a rectangular ribbon of thickness h_{eB} = 0.025 centimeter, the frustrum cut out of the cone by the electron beam has the following dimensions,

H_1 = 0.025 cm, height of frustrum

r_1 = 0.0175 cm, lower radius of frustrum

r_2 = 0.035 cm, upper radius of frustrum

$V = 5.5 \times 10^{-5}$ cm^3, volume of frustrum

$A_B = 2.2 \times 10^{-3}$ cm = V/h, = average cross sectional area of frustrum = average cross sectional area of beam.

Assume that the width of the electron beam equal to the upper diameter of the frustrum, 0.07 centimeter per tube, for the beam cone volume and area as defined,

Molecules/sec in beam = 5.6×10^{12}

Time to traverse frustrum = 5.3×10^{-7} sec

Molecular density = 5.3×10^{10} molecules/cm^3

Assuming a circular array, ten tubes placed so as to produce little or no change in the beam cone as defined, the molecular density is increased by a factor of 10 (5.4×10^{11} molecules/cm^3) and the beam pressure is 1.7×10^{-5}

torr. If 100 tubes are placed in the circular array, the molecular density is 5.4×10^{12} and the beam pressure now is 1.7×10^{-4} torr, as shown in Table 1. Now the ratio of the beam pressure to background is shown as,

$$P_B/P_{BKGD} = S_P/V_B A_B$$

Inserting the values for $S_p = (4 \times 10^3\ cm^3)$, $V_B = (4.76 \times 10^4$ cm/sec), and $A_B = (2.2 \times 10^{-3}$ cm), $P_B/P_{BKGD} = 38$. Thus, the background pressure is 4.4×10^{-6} torr for an array consisting of 100 tubes, which is well within the requirements for the source. The ion current density produced by such a beam is J^+ where,

$$J^+ = J^- \; S \; P_B \; \ell_B \; A/cm^2 \tag{39}$$

In Equation (39),

J^- = Electron current density, A/cm^2

S = Ionization efficiency, $torr^{-1}\ cm^{-1}$

P_B = Beam pressure, torr

ℓ_B = Distance travelled by electron beam through the frustrum, cm. In this case $\ell_{eB} = 1/2\ (D_T + D_B)$ where D_T, D_B are the upper and lower diameter of the frustrum, respectively.

Using $P_B = 1.7 \times 10^{-4}$ torr, and S = 6.5, $J^- = 7.76 \times 10^3$, $\ell_B = 0.05$, $J^+ = 4 \times 10^{-7}$ A/cm for the 100 tube array.

All the data presented in Table 1 was obtained in a manner similar to that detailed above. Specific beam shapes, in terms of relative intensities, are shown in Figure 4. Examination of these figures and Figures 5 and 6 indicate;

$$P_B \propto (L/a)^{-1} \propto J^+$$

$$P_B \propto P_{inlet}$$

The angle within which seventy percent of the molecules reside decreases as the inlet pressure decreases (for a given L/a) and will increase as L/a decreases (for a fixed inlet pressure).

Comparison With Other Source Types

Since the purpose of utilizing the directed gas beam entry source, of the type discussed above, is to maintain or enhance the source ion production characteristics without increasing the pumping requirements of the system, comparison of the results reported with data for other source types should be instructive. The effectiveness in reducing pumping requirements is best illustrated by comparing the directed gas beam entry source with first, an open source, i.e., one which is not conductance limited, but equipped with a gas entry port, not a molecular beam duct array.

The total orifice area for the 100 tube array, cited previously, is $100\ (1.7 \times 10^{-3})\ (\Pi) = 9.07 \times 10^{-4}\ cm^2$. For a hole, the total outflow is given by Equation (8) or (9), with the factor T having the value of one. With the upstream pressure equal to five-tenths of a torr and utilizing nitrogen as the gas, ν, of Equation (9), becomes 1.88×10^{20} molecules per second per unit area and then I_t is 17×10^{16} molecules per second (when $A = 9.07 \times 10^{-4}\ cm^2$). Thus, the total molecular flow for a single ported source is approximately 2×10^2 greater than for the directed entry source based upon 100 tubes.

Obviously, for an ion source of finite dimensions, the pumping requirements of the system would have to be increased in order to maintain the overall source pressure at levels similar to those cited above for the directed beam source. This can readily be seen by application of Equation (11).

Application of Equation (11), utilizing operating conditions similar to those cited for the 100 array directed beam source, shows that for a cone of angular spread of thirty-five degrees, a 5.3×10^{14} molecules/cm^3 density will be achieved. While this represents an increase of 10^2 compared to the 100 tube array source, the P_B/P_{BKGD} ratio is now about 10^4 in order to achieve the same background requirement. Thus, the pump speed, S_p, is now approximately 1×10^6 cubic centimeters per second representing an increase of 2.5×10^2 over that of the directed beam source. For this application, this more than offsets the advantage with respect to the gain in density. Further, by increasing the tube array to 1000, a beam density of slightly less than 10^{14} molecules per cubic centimeter can be achieved and a P_{BKGD} of approximately 10^{-5} torr can still be maintained, utilizing the same S_p of 4×10^3 cubic centimeters per second.

The general relationship between P_B/P_{BKGD} and S_p is shown in Figure 7. This curve was obtained utilizing Equation (33) and V_B, A_B values for the 100 tube array and is valid for an open source, i.e., one that is not conductance limited.

A comparison between the directed beam source and a conductance limited source is also of interest. In this case the relationship is:

$$Q_{source} = P_B A_B V_B = P_{BKGD} C_S = Q_{out} \tag{40}$$

Where C_S is the source conductance. Then

$$\frac{P_B}{P_{BKGD}} = \frac{C_S}{A_V V_B} \tag{41}$$

using values for A_B, V_B, as given above for the 100 array beam source, we see that when $C_S = S_p$ as cited, $P_B/P_{BKGD} = 38$. Now as C_S decreases, by closing the source exit aperture to yield smaller exit aperture areas, P_B/P_{BKGD} will also decrease, due to the rise in background pressure. This relationship is identical to the curve shown in Figure 7 with C_S replacing S_p on the ordinate of the graph.

The comparison between the direct gas beam entry source and a conductance limited source, relative to the ion current density produced by each, is also of interest. The conductance limited type source is the differential pumped ion type source currently employed by many mass spectrometric systems.

For a differentially pumped ion source, the ion current density at the ion exit aperture can be shown as J^+_{DP}, where

$$J^+_{DP} = \frac{0.332 \times 10^{-4} S Q J^- \ell_{eB} (h_b + W_b) \ell_b^2}{h_b^2 W_b (\ell_B W_B)} \tag{42}$$

where Q is the gas flow through the source, torr - cm^3/sec

S and J^+ are as previously defined

W_b = Width of electron entrance aperture

ℓ_{eB} = Length of electron entrance aperture

ℓ_b = Distance electron travels through beam

h_b = Thickness of electron beam, height of electron entrance slot

$(\ell_B W_B)$ = Area of ion exit aperture

Similarly, for a direct gas beam entry source the ion current density at the ion exit aperture can be shown as J^{+}_{DE}, where

$$J^{+}_{DE} = \frac{2.2 \times 10^{-5}\ S\theta J^{-}\ \ell_b^{\,2}\ W_b}{A_B\ (W_B\ \ell_B)} \tag{43}$$

with all terms as previously defined.

The ratio of Equations (42) and (43) yield the desired comparison, namely

$$\frac{J^{+}_{DP}}{J^{+}_{DB}} = \frac{1.5\ \ell_{eB}\ A_B\ (h_b + W_b)}{h_b^{\,2}\ W_b^{\,2}} \tag{44}$$

where $\ell_{eB} = 2.5 \times 10^{-3}$ cm

$A_B = 22 \times 10^{-3}$ cm^2

$h_b = 0.025$ cm

$W_b = 0.07$ cm

and,

$$\frac{J+_{DP}}{J^{+}_{DB}} = \frac{4 \times 10^{-6}}{3 \times 10^{-6}} = 1.33 \tag{45}$$

Hence, the ion current density achieved by using a conductance limited source with the above ℓ_{eB} value is only slightly greater than that produced by an appropriate direct gas entry source, while the latter greatly reduces the pumping requirements of the system and still yields a comparable gas density in the source. An increase in the value of ℓ_{eB} will increase the ratio value. However this will also have the undesirable effects noted in previous sections.

The following conclusions may be drawn based upon the work conducted to date: First, a direct gas beam entry source is feasible, second, utilization of an array of tubes at low inlet pressures will lead to relatively large gas densities in the ionizing region of the source, third, the direct gas beam entry source compares favorably with respect to the differentially pumped ion source, and fourth, present ion source pumping requirements will not be exceeded through application of the direct gas beam entry source.

DIRECT ENTRY FROM AN ACCUMULATOR CELL

The design of a micro accumulator cell system is examined to determine whether it is feasible and advantageous to permit the entire effluent from the cell to flow through the mass spectrometer during determination of trace contaminants in the atmosphere.

The latter system is presumed to have an atmospheric or low conductance leak. The points of particular interest in this analysis are the sensitivity for detection, identification of contaminants and the costs in terms of weight and power for the particular system.

In earlier studies with the Laboratory Contaminant Sensor System, relatively large sorbent cells were employed and as the concentrated contaminants were desorbed by heating the cell they were continuously pumped away from the inlet system through a bypass pumping line. A theoretical model for this desorption mode was developed which described the system at least quantitatively. In the Molecular Beam Direct Entry Ion Source Section, Page 7, this model is applied to the system in which the total flow of contaminants is carried by the mass spectrometer alone. This necessarily involves a reduction in size of the system since the gas load that the mass spectrometer pump can handle is limited. In the following analysis it is assumed that an instrument of the Mass Spectrometer Atmospheric Sensor type, with a miniaturized ion pump, is employed for the analysis, at least insofar as the pumping system is involved.

System Analysis

In the accumulator cell system, for analysis of trace contaminants, there are five variables that determine the performance of the system for trace contaminant analysis. These are:

(1) The equilibrium constant

(2) The heat of desorption

(3) The weight of sorbent in the cell

(4) The rate at which the cell is heated

(5) The contaminant removal rate.

The first two variables are characteristics of the sorbents used and the contaminants, and the latter three are system design variables.

Sorbents are chosen for the analysis of certain types of contaminants on the basis of the equilibrium constant and the heat of desorption of these contaminants in the sorbent. The equilibrium constant and heat of desorption are defined for the following reaction:

$$\text{Contaminant} \cdot \text{Sorbent} \rightleftarrows \text{Contaminant (g)} + \text{Sorbent}$$

The equilibrium constant is

$$K = \frac{p}{c}$$

where p = Pressure of the contaminant in the gas phase

c = Concentration of contaminant on the sorbent

For the reaction as written above, the heat of desorption is the amount of energy required to desorb the contaminant from the sorbent.

The choice of sorbent is guided by two considerations. First, the equilibrium constant at room temperature must be sufficiently small so that the contaminant is essentially completely sorbed at room temperature and is not lost in the precut or purge operation used to remove residual air from the system. Stated another way, the pressure of the contaminant in equilibrium with the sorbent must be very small at room temperature. The second consideration is that, at the highest temperature at which the sorbent can be used, the equilibrium constant must be large enough so that the contaminant can be removed completely from the sorbent. This implies that the heat of desorption has a value such that the change in equilibrium constant with temperature, which is governed by the following relation

$$\frac{d \ln K}{dT} = \frac{\Delta H}{RT^2}$$

will be sufficient to meet this criteria. The maximum temperature at which a sorbent can be used is considered to be that temperature at which side reactions begin to interfere with the determination of contaminants. For Porapak Q, a sorbent used in the Laboratory Contaminant Sensor Studies, this

temperature is about 230 degrees centigrade; above this temperature, thermal degradation of the polymer produces compounds which have mass spectral patterns that interfere with determination of certain contaminants. For charcoal, the thermal stability is not a particular problem but reactions with residual oxygen in the system may result in interferences in the determination of certain contaminants.

The equilibrium constant and the heat of desorption are not design variables for the system except insofar as the selection of a given solvent for the analysis of certain contaminants is a design variable.

The system design variables are first, the weight of sorbent and the volume of the cell; second, the heating rate; and third, the contaminant removal rate, either by carrier gas or vacuum operation. Within certain limits, the values of these variables can be chosen to achieve a desired performance in the analysis. The choice of these variables is governed in part by the characteristics of the mass spectrometer, the sample size and the mode of operation selected. Final selection of the complete system, including the design variables and mode of operation, will be based on considerations of weight and power. The effect of the system variables on the analytical characteristics is reviewed in the following paragraphs and the total system design is considered subsequently.

Two characteristics, the desorption temperature and the sensitivity, used in the analysis of contaminants are dependent on the system variables and the sorbent characteristics. Desorption of contaminants under vacuum operation is described by the following differential equation:

$$\frac{dp}{dt} = \frac{p}{V + \frac{w}{K}} \left\{ -kp + \left(V + \frac{w}{K} \right) \frac{\beta}{T} + \frac{\Delta H}{RT^2} \frac{w}{K} \beta \right\} \tag{46}$$

p = Pressure due to contaminant desorption

t = Time

V = Volume of the system

w = Weight of sorbent

K = Equilibrium constant

k = Conductance out of the system

T = Temperature (°K)

β = Heating rate

ΔH = Heat of desorption

R = Gas Constant

The temperature at which the maximum desorption rate occurs in the desorption curve is approximated by ignoring the second term in Equation (46) above. The condition at this maximum is $\frac{dp}{dt} = 0$ which implies

$$\frac{\Delta H}{RT_m^2 K_m} = \frac{k}{w\beta} \tag{47}$$

where the subscript m denotes the value at the temperature of maximum desorption pressure.

It can be shown that the temperature of maximum desorption pressure is not a very sensitive function of the system variables. Thus, the value of the equilibrium constant at that temperature is given by

$$K_m = K_o \exp\left\{\frac{-\Delta H}{R}\left(\frac{1}{T_m} - \frac{1}{T_o}\right)\right\} \tag{48}$$

where the subscript o refers to initial conditions (temperature approximately 25°C). Rewriting Equation (47) with this substitution

$$\ell n \frac{\Delta H}{R} - 2\ \ell n\ T_m - \ell n\ K_o + \frac{\Delta H}{RT_m} - \frac{\Delta H}{RT_o} = \ell n\ k - \ell n\ w - \ell n\ \beta$$

from which the rate of change of T_m with heating rate β, for example, is

$$\frac{dT_m}{d\beta} = \frac{T_m/\beta}{\left(2 + \frac{\Delta H}{RT_m}\right)} \tag{49}$$

For values of ΔH in the range of ten kilocalories per mole, an increase in the heating rate by a factor of two results in an increase of T_m by about thirty-five degrees centigrade at 250 degrees centigrade. Similar considerations apply to the other system variables. What this means is that the desorption characteristics are more dependent on the sorbent-sorbate physical chemical properties than on the system design.

The sensitivity of the system for detection of trace contaminants should rigorously be derived by numerical integration of Equation (46) above. The sensitivity can be measured either in terms of the area under the desorption curve or the pressure at the maximum in the desorption curve. In the Laboratory Contaminant Sensor program the peak maximum was used as the measure of the amount of contaminant present and this seems to afford the simplest measure from the point of view of automated data handling.

An approximation to the peak maximum pressure can be derived by equating the area under the desorption curve to the total amount of contaminant sorbed, on the assumption that the desorption curve can be represented as a triangle. Thus, the area under the curve is

$$\text{Area} = \frac{p_{max}\ \Delta T_{1/2}\ k}{\beta}\ \frac{T_o}{T_m} = S \tag{50}$$

p_{max} = Pressure at the peak of the desorption curve

$\Delta T_{1/2}$ = Width of the peak (°K) at half the peak maximum value

k = Conductance

β = Heating rate

S = Total sample in appropriate units

Rearranging this equation yields

$$\frac{p_{max}}{S} = \frac{\beta}{\Delta T_{1/2}\ k}\ \frac{T_m}{T_o} \tag{51}$$

which provides the maximum pressure per unit sample sorbed. Now $\Delta T_{1/2}$ in this expression will depend on the heat of desorption; however, experience with the Laboratory Contaminant Sensor System and theoretical studies in the literature indicate that for the range of ΔH values encountered in the analysis of contaminants, $\Delta T_{1/2}$ is on the order of seventy to eighty degrees centigrade. The controlling variables are therefore, the ratio of β/k. It is interesting to note that the sensitivity for all contaminants will be approximately the same (except for differences in mass spectral sensitivities) as long as $\Delta T_{1/2}$ is the same.

The above equations apply to a system operated with vacuum pump out to remove the contaminants as they desorb. In the derivation of the equations, it is assumed that molecular flow conditions apply during pump out. If the flow is viscous, the removal rate of any individual contaminant will depend on the total pressure in the system; that is, k in the derived equations will be replaced by k'pT. If an inert carrier gas is used to remove the contaminants as they desorb, the equations are exactly the same as those derived above except in this case k represents the carrier gas flow rate.

Total System Considerations

Various systems have been considered for the flight trace hardware. Summarized briefly, these include: first, operation similar to the Laboratory Contaminant Sensor System with vacuum precut and bypass pumping; second, operation with pumping only from the mass spectrometer vacuum after an initial precut of residual air with a syringe type pump; and third, operation with a slow flow of carrier gas to remove the contaminants as they desorb.

The first two systems are used with a mass spectrometer equipped with a high conductance leak, and the third would be used with a low conductance, or atmospheric pressure leak. In addition to the three systems listed above, two operational options may be considered. The first is operation without temperature programming; that is, operation with the heating rate that results from instantaneous input of the total power necessary to maintain the temperature at the highest required value, generally about 250 degrees centigrade. Another option is in the sampling technique; the analysis may be performed by selecting a sample volume such that the sorbent is saturated with the various contaminants, or by choosing a sample volume that will not saturate the sorbent for the least tightly sorbed contaminant that can be detected on a given sorbent. The choice between these systems and operational modes depends on the tradeoff between sensitivity for contaminant detection and weight and power required for the operational mode selected, and must be governed in part by the anticipated analytical problem.

The anticipated analytical problem has important implications in the selection of the heater operational mode. The two options to be considered are: First, applying full power to the heater and allowing the temperature to increase to its final value at an essentially uncontrolled rate or, second, controlling the power input to the heater in order to control the temperature rise rate at some predetermined value. The latter mode requires

additional power to operate a controller unit and is, therefore, less desirable from the flight system weight and power constraints. If full power is applied directly to the heater at the start of the analysis, the initial temperature will rise rapidly and approach the selected final temperature asymptotically. Unless a very high contaminant removal rate is available (either high carrier gas flow or pump speed), the contaminants will all desorb and be present in the vapor phase simultaneously, and the separation achieved by controlling the ratio of k/β will be lost. If there are many contaminants present in the atmosphere in significant amounts, the resulting mass spectra will be difficult to interpret. If only a few contaminants are present, the loss of resolution during desorption will be of less consequence since it should prove feasible to identify mixture components by their mass spectra. An advantage to the rapid heating rate approach is that the maximum sensitivity is achieved for a given amount of sample (β/K large in Equation (51)). This enhanced sensitivity in desorption could be traded for increased identification capability if low voltage ionization is utilized for the mass spectra. There are other features of this mode of operation that should be explored more fully in the final selection of a Flight Trace Contaminant System. For example, the precut must reduce the pressure to a relatively low value for a sorbent, such as charcoal, which retains a large amount of air and water in order to avoid excessively high pressures in the ion source for rapid heating of the cell. For the present, it is sufficient to point out that this mode of operation eliminates the requirement for a temperature programmer controller, at the expense possibly of complete identification of contaminants.

Operation in the Saturation Mode

The preceding discussion and calculations relate to operation in a mode in which a fixed sample volume is passed through the sorbent. The sorbate-sorbent characteristics determine which contaminants will be retained during removal of air and which will be substantially lost in the precut or purge operation. As an alternative it is possible to use a sample volume that will saturate the weight of sorbent chosen for the cell. This volume should be that which is required to saturate the sorbent for the most tightly held contaminant which can be desorbed from that sorbent. This mode of operation has the effect of reducing the sensitivity for the less strongly sorbed contaminants.

In the relation between maximum desorption pressure and sample of contaminant

$$\frac{p_{max}}{N_o} = \frac{\beta}{\Delta T_{1/2}\, k}$$

the total sample N_o which is given by

$$N_o = V_s\ p$$

(where V_s represents the volume of sample)

in the undersaturated mode is replaced by

$$N_o = p_o\ \frac{w}{K_o}$$

where

$$K_o = \frac{p}{C_s}$$

for operation in the saturated mode. For the same concentration p_o, in the gas phase, relatively larger quantities are sorbed at saturation for contaminants which are strongly sorbed (K_o very small).

$$\frac{p_{max}}{p_o} = \frac{\beta}{\Delta T_{1/2}^{\ k}}\ \frac{w}{K_o}\ ,$$

which shows the decrease in sensitivity for contaminants with large values of K_o.

The other factor to be considered in using saturation samples, is the possible nonlinearity of the sorption isotherm. In general, nonlinearity in the isotherm implies that K_o is dependent on p_o, and in most cases K_o decreases with decreasing p_o; or stated simply, relatively larger amounts of contaminant are sorbed at lower partial pressures of contaminant. This has the effect of increasing the sensitivity at low concentrations of contaminants, which would be advantageous if sensitivity is a limiting factor.

If the isotherms should prove to be nonlinear, operation in either mode would require extensive calibration for very low level contaminants. Past experience has indicated that for some of the compounds sorbed on Porapak Q there may be some nonlinearity in the isotherm. However, the experimental data available is not sufficient to establish this unequivocally, since some other sorption process in the inlet system (on the wall perhaps) could also account for the observed phenomena.

At present, it appears that operation in the undersaturated mode is more attractive since approximately the same sensitivity (except for inherent differences in mass spectral sensitivity) could be attained for almost all compounds in the programmed temperature desorption mode. If full power heating is employed, so that only a very small amount of the sample is removed during the actual cell heating, the accumulator cell system will have increased sensitivity for less tightly sorbed contaminants.

Desorption Pressure Requirements - Inlet Leak Considerations

The system design requires that over the contaminant concentration range of interest, the desorption pressure is high enough to yield a measurable signal over the system background. For the three systems considered above, this requirement imposes the tightest constraint on the second system, in which the total contaminant sample must be pumped off through the mass spectrometer. In this case, both the maximum pressure and the total sample of contaminants must be matched to the inlet leak and pumping speed of the mass spectrometer.

Considering a mass spectrometer of the atmospheric sensor type, the instrument background levels at present appear lower than the noise and drift level of the detector, which is in the range of 10^{-14} amperes. On the basis of calculation from the Laboratory Contaminant Sensor Studies, it also appears that the cell background levels would be below this value.

In these studies, no signal was observed above the background of the instrument when blank or contaminant-free samples were analyzed. For that system therefore, the inlet system pressure, due to contaminants and related to the sample, under normal operating conditions was less than 10^{-5} torr. Relating this to an Atmospheric Sensor Mass Spectrometer System with an inlet leak conductance of 0.01 cubic centimeter per second and source sensitivity of 1×10^{-6} amperes per torr, this is equivalent to an ion current of less than 10^{-14} amperes. It may be possible, under conditions of maximum sensitivity, that a measurable cell background will be detectable but this must be established experimentally under the existing operating conditions. At present, it appears that the detector drift levels will be the limiting factor.

An ion current of 10^{-13} amperes should provide an adequate signal for measuring the base mass peak (m/e) for a contaminant at the lower end of the concentration range. This would permit important fragment ions to be detected for identification of the contaminant. Assuming a range of detection for contaminants from one-tenth to ten parts per million, an ion current of 10^{-13} amperes would correspond therefore to one-tenth part per million and 10^{-11} amperes to ten parts per million for linear response over this range.

The full dynamic range of a mass spectrometer of this type would permit ion currents up to 10^{-10} amperes to be utilized without over-pressurizing the ion source. Choice of 10^{-11} amperes as the upper limit for the contaminant analysis range, allows for the possibility that several contaminants may be present in the source simultaneously so that the total source pressure, even in this instance, would not exceed the maximum of the linear range of source operation.

The inlet system pressure required to yield an ion current of 10^{-13} amperes at the peak of the desorption curve depends on the leak conductance. The relationship is

$$p_i = \frac{c_s S I^+}{C_L}$$

p_i = Pressure in the inlet system

c_s = Source conductance, 40 cc/sec for MSAS

S = Sensitivity of the (amps/torr)

C_L = Conductance of the leak

For an ion current of 10^{-13} amperes, and leak conductance of one-tenth of a cubic centimeter per second, an inlet system pressure of 4×10^{-4} torr is required from a sample containing one-tenth of a part per million contaminant. This calculation is based on the assumption that the mass spectrometer has equal sensitivity for the contaminant and nitrogen; the data used apply to nitrogen.

Accumulator System

From the design equations presented earlier, the system parameters are calculated for a cell that will yield a pressure of 4×10^{-4} torr from a sample of gas containing one-tenth part per million of contaminant on an appropriate sorbent. Considering first Equation (51), which relates the sensitivity, and assuming that the cell is operating in an undersaturated mode, provides

$$\frac{\beta}{k\ \Delta T_{1/2}}\ \frac{T_m}{T_o} = \frac{p}{S} = \frac{4 \times 10^{-4}\ \text{torr}}{V_S\ (\ell) \times 0.1 \times 10^{-6}\ \frac{\text{atm}}{\text{atm air}}\ \frac{760\ \text{torr}}{\text{atm}} \times 10^3\ \frac{\text{cc}}{\ell}}$$

$$= \frac{0.525 \times 10^{-2}\ \text{torr}}{V_S\ \text{torr-cc}}$$

For $k = C_L = 0.01$ cubic centimeters per second or six-tenths of a cubic centimeter per minute

$$\frac{\beta}{k\ \Delta T_{1/2}}\ \frac{T_m}{T_o} = \frac{0.525 \times 10^{-2} \times 0.6}{V_S\ (\ell)} = 0.315 \times 10^{-2}$$

and for $\Delta T_{1/2}$ on the order of 100 degrees centigrade, and a sample volume of 0.05 ℓ

$$\beta \left(\frac{T_m}{T_o} \right) = 6.3°C/\text{min}$$

For smaller sample volumes a faster heating rate can be employed.

The next factor to be considered is the temperature at which the maximum in the desorption curve occurs. This is given by

$$\frac{\Delta H}{RT_m^2\ K_m} = \frac{k}{w\beta}$$

In order to evaluate this expression, ΔH and K values taken from the gas chromatographic data for toluene will be used, it will be assumed that T_m is on the order of 200 degrees centigrade, the value found in the Laboratory Contaminant Sensor Studies.

ΔH for toluene on Porapak Q is about 12,000 calories per gram-mole and K_m is 0.033 grams per cubic centimeter at 200 degrees centigrade.

$$\frac{k}{w\beta} = \frac{12{,}000}{1.986 \times (473)^2 \times 0.033} = 0.81\ \frac{\text{cc}}{°C\text{-g}}$$

for k and β chosen above

$$w = \frac{0.60 \text{ cc/min}}{3.9 \text{ °C/min} \times \frac{.81 \text{ cc}}{\text{°C-g}}} = 0.19 \text{ g}$$

which is not an unreasonable value. It should be pointed out, that if a smaller sample is chosen in order to be able to increase the heating rate and speed up the analysis, the weight of sorbent must be reduced or a higher desorption temperature will result.

In order to insure that the sample volume will not saturate this weight of sorbent, the saturation volume is calculated from the initial value of K_o, which for toluene on Porapak Q is 1.4×10^{-5} grams per cubic centimeter. The volume required to saturate 0.41 grams of Porapak Q with toluene at one-tenth part per million is

$$V_S = \left(V_g + \frac{w}{K}\right) \approx \frac{w}{K} = \frac{0.19}{1.4 \times 10^{-5}} \text{ cc} = 1.4 \times 10^4 \text{ cc}$$

which is well above the fifty cubic centimeter volume chosen.

As a further test of these equations, and this design, the desorption temperatures for other compounds for which gas chromatographic data is available may be calculated. For example, for hexane ($K_o = 8.4 \times 10^{-5}$, $\Delta H = 11{,}000$ calories per mole)

$$T_m^2 \; K_o \exp\left[-\frac{\Delta H}{R}\left(\frac{1}{T_m} - \frac{1}{T_o}\right)\right] = \frac{11{,}000 \times 0.21 \times 3.9}{2 \times 0.6} = 7.5 \times 10^3$$

$$T_m \approx 175°C$$

and for methyl acetate ($K_o = 2.44 \times 10^{-4}$, $\Delta H = 10.2$),

$$T_m \approx 155°C$$

These values indicate that in general the performance of this system would parallel fairly closely that of the Laboratory Contaminant Sensor.

One other factor to be considered is the precut required to reduce the total pressure to a value such that the ion pump capacity would not be overloaded. For this system, assuming a 0.01 cubic centimeter per second

inlet leak conductance, a forty cubic centimeter per second source conductance, and a maximum source pressure of 1 x 10^{-4} torr, the maximum pressure which can be tolerated in front of the leak is four-tenths of a torr. Some external means of reducing the pressure to about two-tenths of a torr is necessary to operate the system in this mode. A syringe type pump might satisfy this requirement. Depending on the sorbent or the amount of air held up on the sorbent and the volume of the system, the leak and the pumping capacity of the ion pump should be capable of maintaining this pressure within limits. This aspect of the operation should be verified experimentally, particularly for a sorbent such as charcoal, which tends to retain large quantities of air and water.

It is also interesting to note that if a leak of very low conductance is used in place of the 0.01 cubic centimeter per second leak in the calculations described above, the heating rate required to give the sensitivity does not change but the peak maximum temperature increases to a much higher value. However, if the ratio of the leak conductance (C_L or, in this closed system or the pump speek k) to the weight of sorbent is kept constant, the same desorption temperature should result. Rearrangement of the sensitivity equation yields the following result:

$$\frac{p_m C_L}{X} = \frac{\beta}{\Delta T_{1/2}} \frac{T_m}{T_o}$$

but in this equation pC_L is just the flow through the ion source (or the mass spectrometer) required to give the desired sensitivity at the desorption peak maximum. Thus if C_L is reduced, the pressure needed increases but the product of the two remains constant. The temperature at which the peak maximum occurs depends on the ratio of k/w, so that by scaling these variables together, the same desorption curve is obtained.

For the system design, the minimum heater power will be determined by the amount of sorbent in the system, provided the auxiliary connecting lines and valves are relatively small or not heated. In this case there are three limitations that must be considered to set a minimum on the sorbent weight. These are: First, there must be sufficient sorbent to permit good contact with a representative sample of gas; second, the system volume relative to the weight of sorbent must not be excessive; and third, the conductance, which is scaled to the sorbent weight, must be high enough, or alternately, the precut level must be low enough so that the residual gas in the system, when heated at the determined rate, will not exert so high a pressure in the system as to overload the ion source. The volume restriction is not stringent unless very small weights (1 mg) of sorbent are considered. The system volume does not become important in determining the desorption curves unless

the ratio of V/w approaches ten to twenty percent of the value of $\Delta H/RK_m T_m$, which in the calculations above is on the order of 400 cubic centimeters per gram. The conductance of the system cannot be reduced to such a low value, or the total pressure in the system cannot be so high that the flow of gas from the cell to the leak becomes diffusion limited. Thus, the leak conductance must be a finite value sufficient to transport the desorbing gases from the cell. This value depends in part on the available precut pump and on the geometry of the inlet system.

Time Period for Analysis

Minimum interval for analysis is determined by the time required for heating and cooling the sorbent cell, or cells. The sampling time would be relatively short compared to these values. At a heating rate of approximately four degrees centigrade per minute, the time for desorption is about one hour; the cooling time is estimated at about twenty minutes, assuming that sample flow can be used to cool the cell once a temperature below seventy-five degrees centigrade is reached. If three cells are used for analysis of the various contaminants, this implies a minimum analysis time of three hours and twenty minutes for programmed temperature desorption, at the rate selected above, to give the desired sensitivity and peak maximum temperature. The heating rate can be increased to increase the sensitivity with perhaps some loss in separation. If the temperature programming is eliminated and the system operated with full power heating immediately the full cycle time can be significantly reduced. A five minute heating time per cell would give a total cycle time of about forty-five minutes.

CONCLUSIONS

In conclusion, the theoretical analysis carried out on this program indicates that the Direct Entry Accumulator Cell and the Molecular Beam Ion Source have promise as basic elements of the Flight Trace Contaminant Analyzer. Experimental verification of the advantages of the molecular beam source would be necessary before a commitment to this design approach could be made. In particular the construction of the array of channels required for the formation of the beam and the close placement of the electron beam to the sample inlet must be resolved.

Some experimental effort has already been carried out toward the Direct Entry Accumulator Cell concept as part of the Carbon Monoxide Accumulator Cell effort, but a low pressure, direct entry system has not been tested. Smaller accumulator cells have been shown to give comparable performance to their larger fore-runners, and further reduction of cell size, in conjunction with the direct entry approach, is a step in the right direction insofar as power, weight and size saving is concerned. If it is desirable to eliminate the need for a pump out line by utilization of direct sample entry, then it will be necessary to devise a means of evacuating the small cell volume during the precut phase. On the other hand, even if a pump out line is utilized for the vacuum precut the smaller accumulator cell size associated with the utilization of the entire sample by the mass spectrometer is desirable.

THIS PAGE INTENTIONALLY LEFT BLANK

REFERENCES

1. Clausing, P., "Uber die Stromung sehr verdunnter Gase durch Rohren von heliobeger Lunge", Annalen der Physik 5, No. 12, pp 961-989 (1932).

2. "Kinetic Theory of Gases", L.B. Locke, 34d Edition, Buer Publications Inc., N.Y., 1961.

3. "Scientific Foundations of Vacuum Techniques", Dushman, S., and Lafferty, J.M., 2nd Edition, J. Wiley and Sons, Inc., N.Y., 1962.

4. "Molecualr Beams", Ransey, N.F., Oxford Press (England), 1956.

5. "Molecular Beam Sources Fabricated From Multi-Channel Array"; "I. Angular Distributions and Peaking Factors", Jones, R.H., et al., Appl. Physics, Vol 40 (11), 4641-4649 (1964).

6. "Molecular Beam Formations by Long Parallel Tubes", Giordmain, J.A., Wang, T.C., "Journal of Applied Physics", V. 31, No. 3, pp 463-71 (1960).

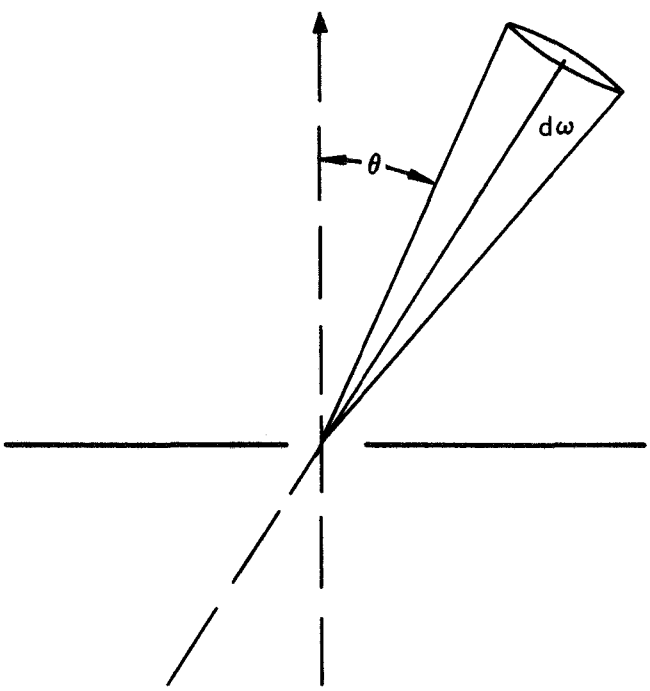

FIGURE 1.- Angular Effusion of Molecules from Orifice

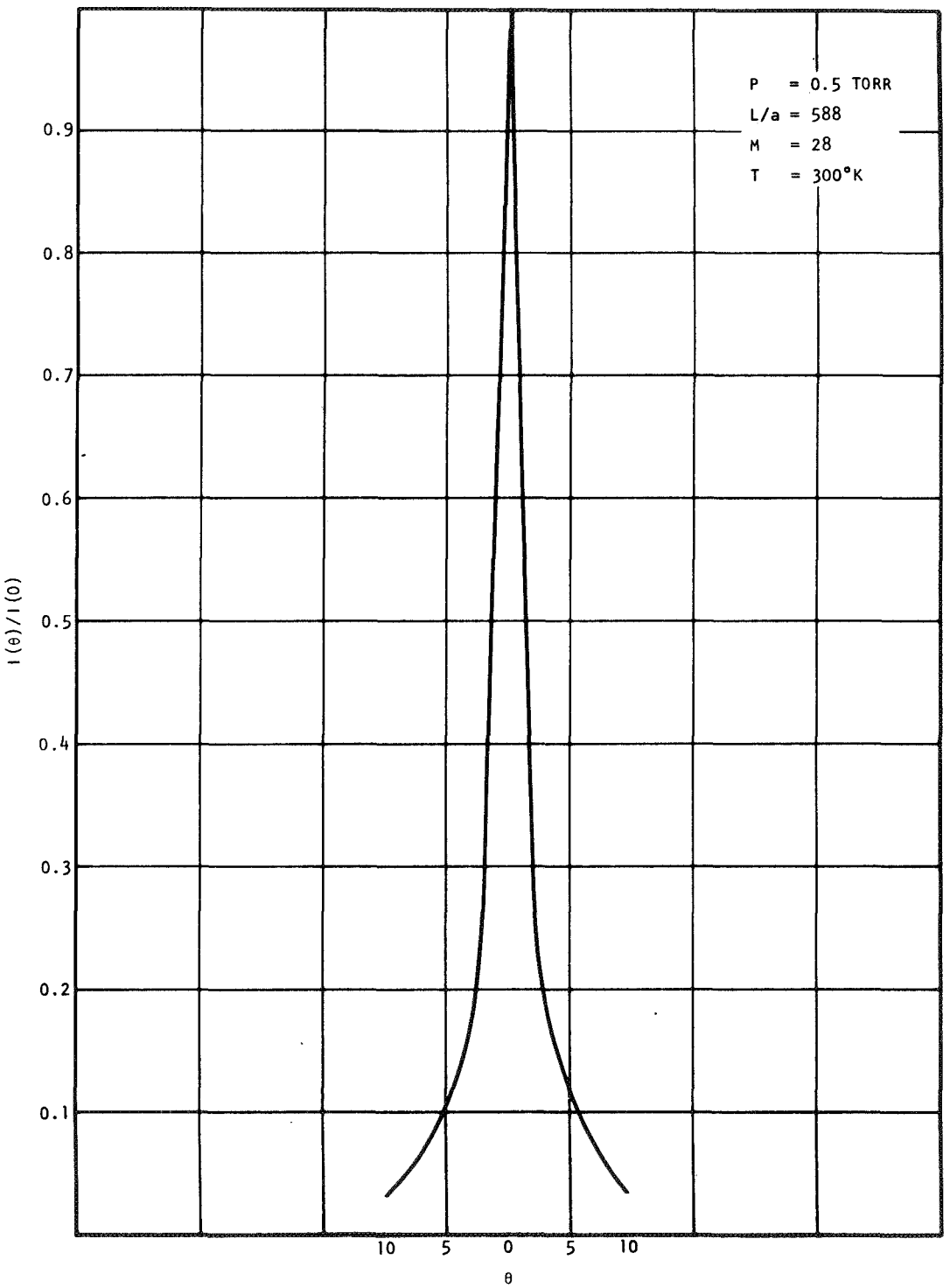

FIGURE 2.- Beam Shape Curve

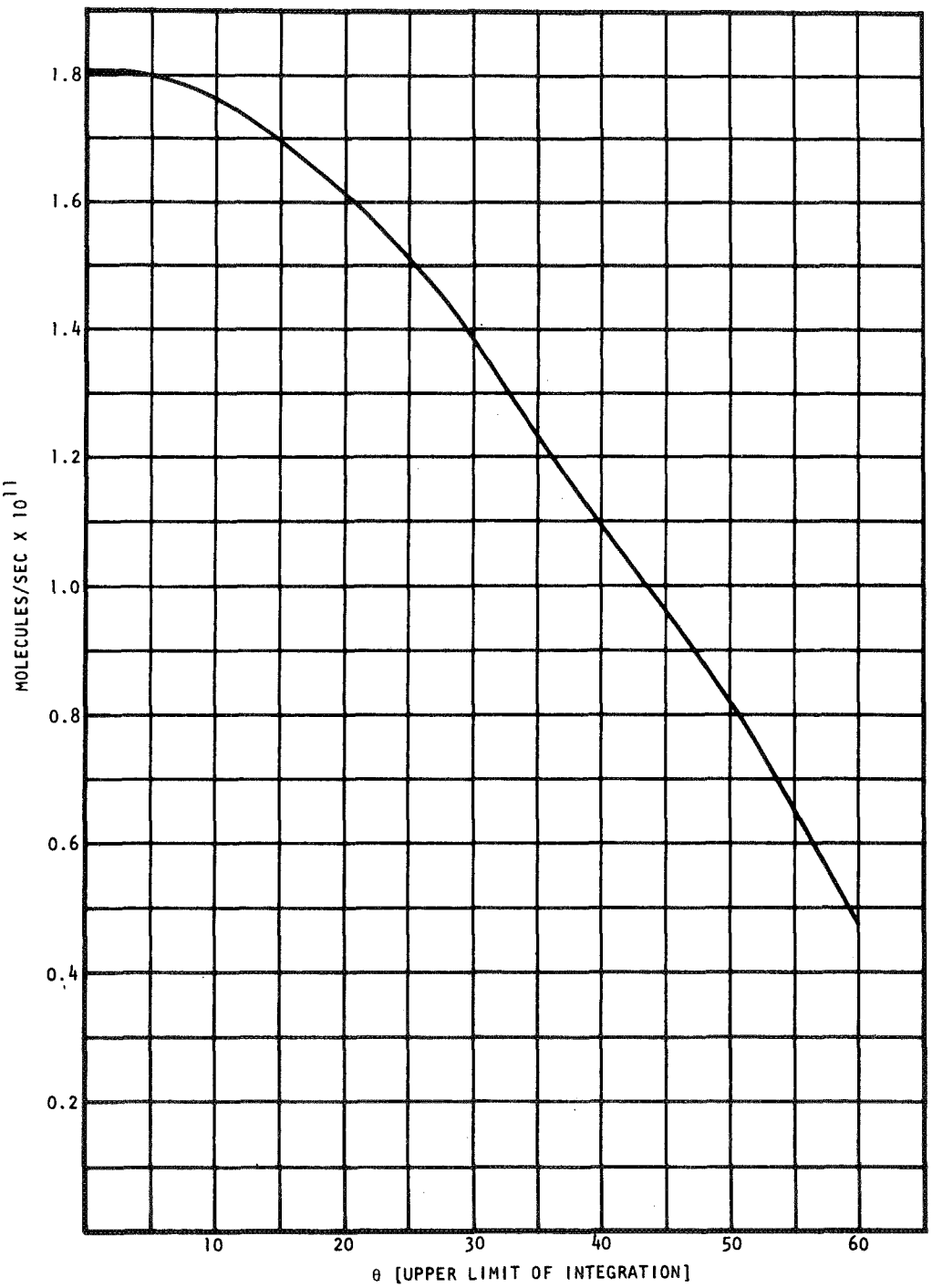

FIGURE 3.- Molecular Distribution for Beam With L/a 588

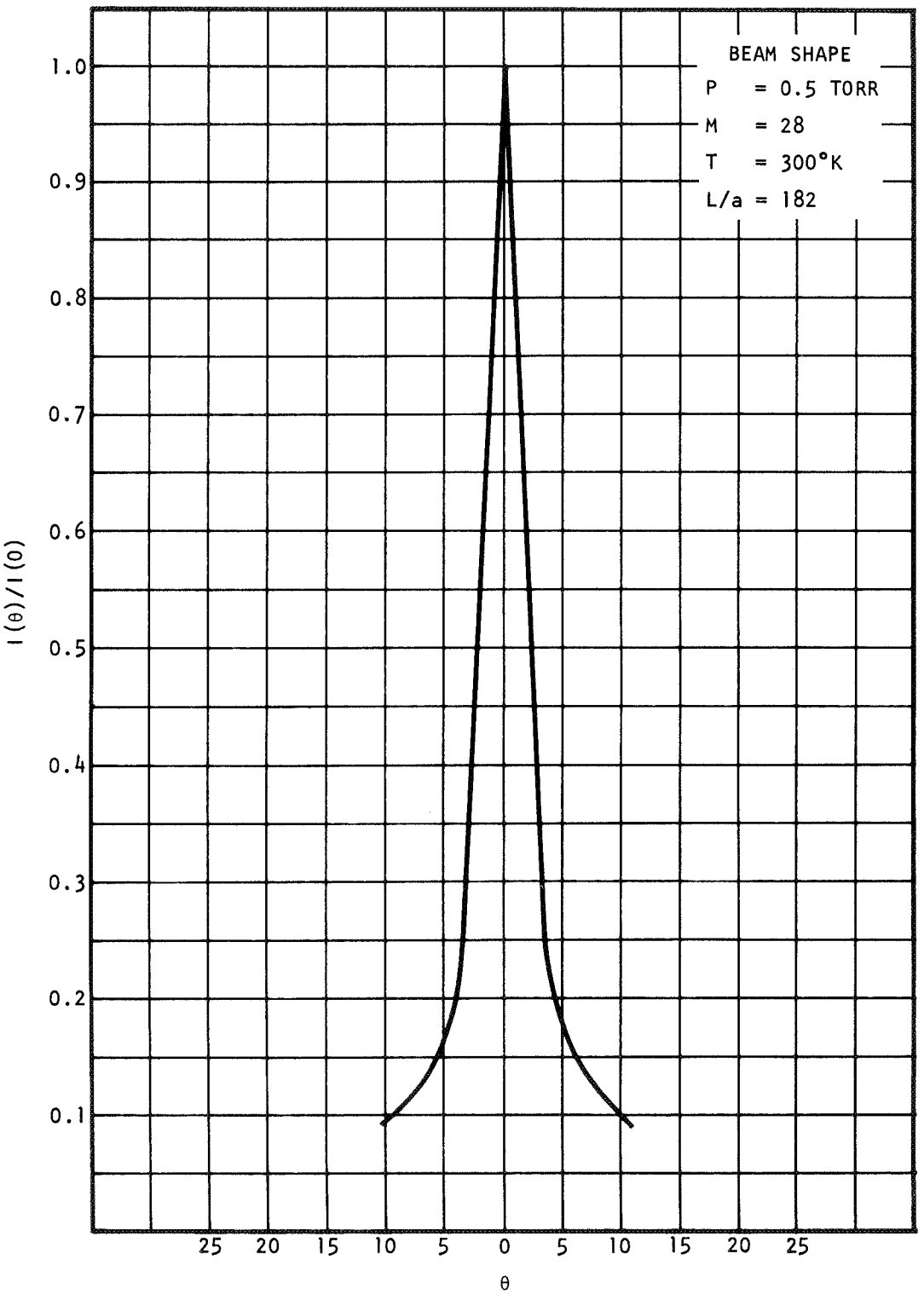

FIGURE 4.- Beam Shapes in Terms of Relative Intensities (Sheet 1 of 4)

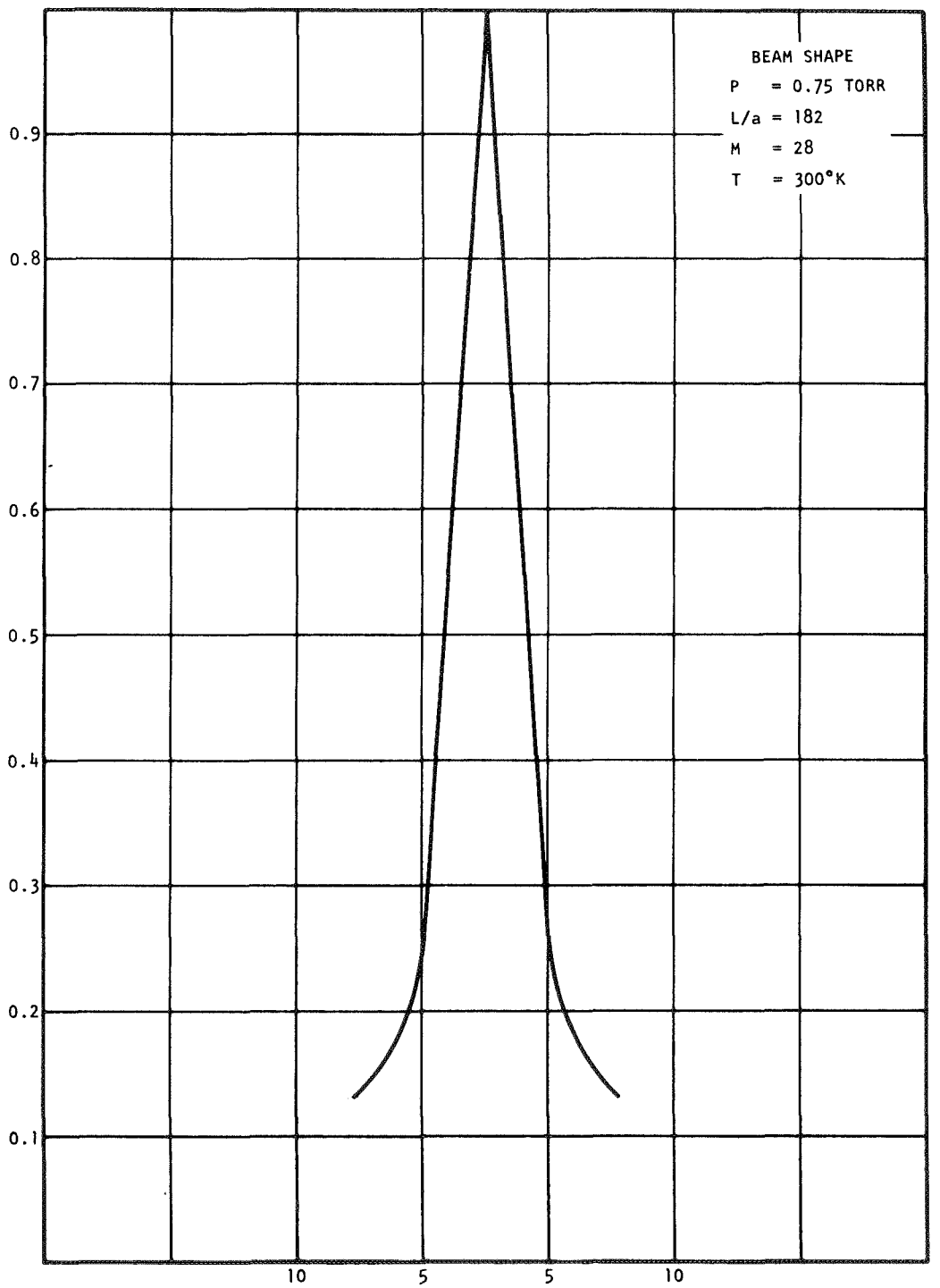

FIGURE 4.- Beam Shapes in Terms of Relative Intensities (Sheet 2 of 4)

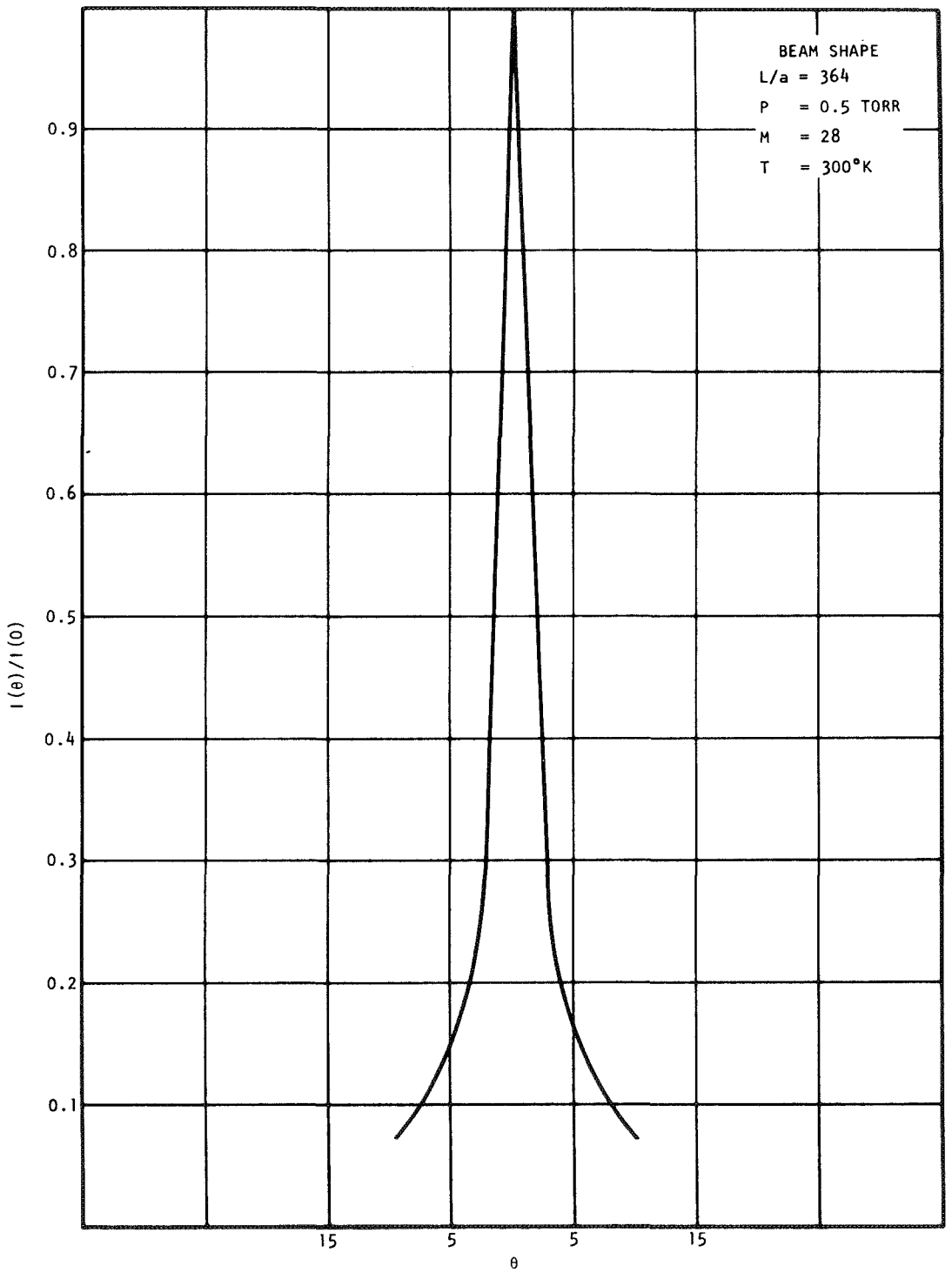

FIGURE 4.- Beam Shapes in Terms of Relative Intensities (Sheet 3 of 4)

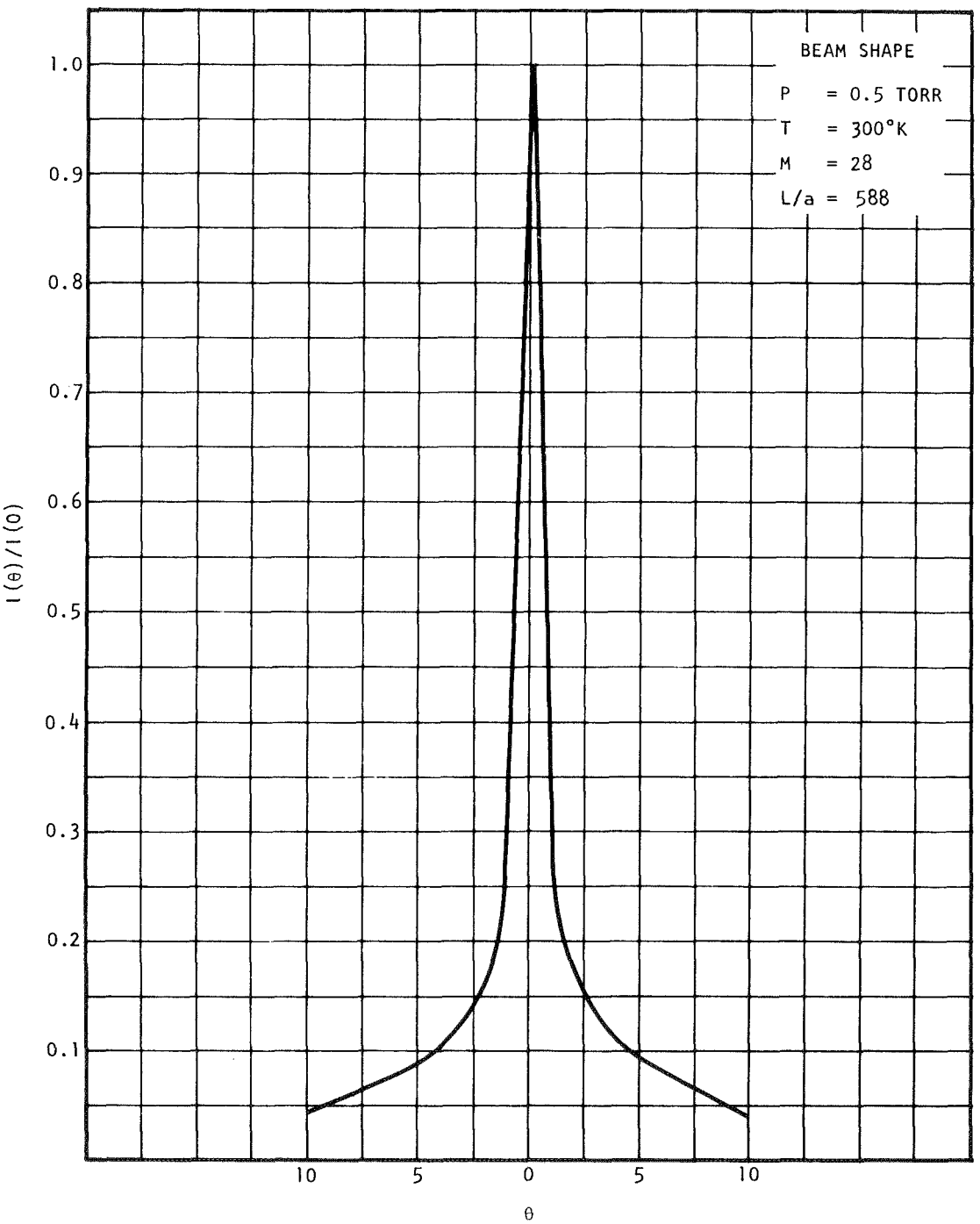

FIGURE 4.- Beam Shapes in Terms of Relative Intensities (Sheet 4 of 4)

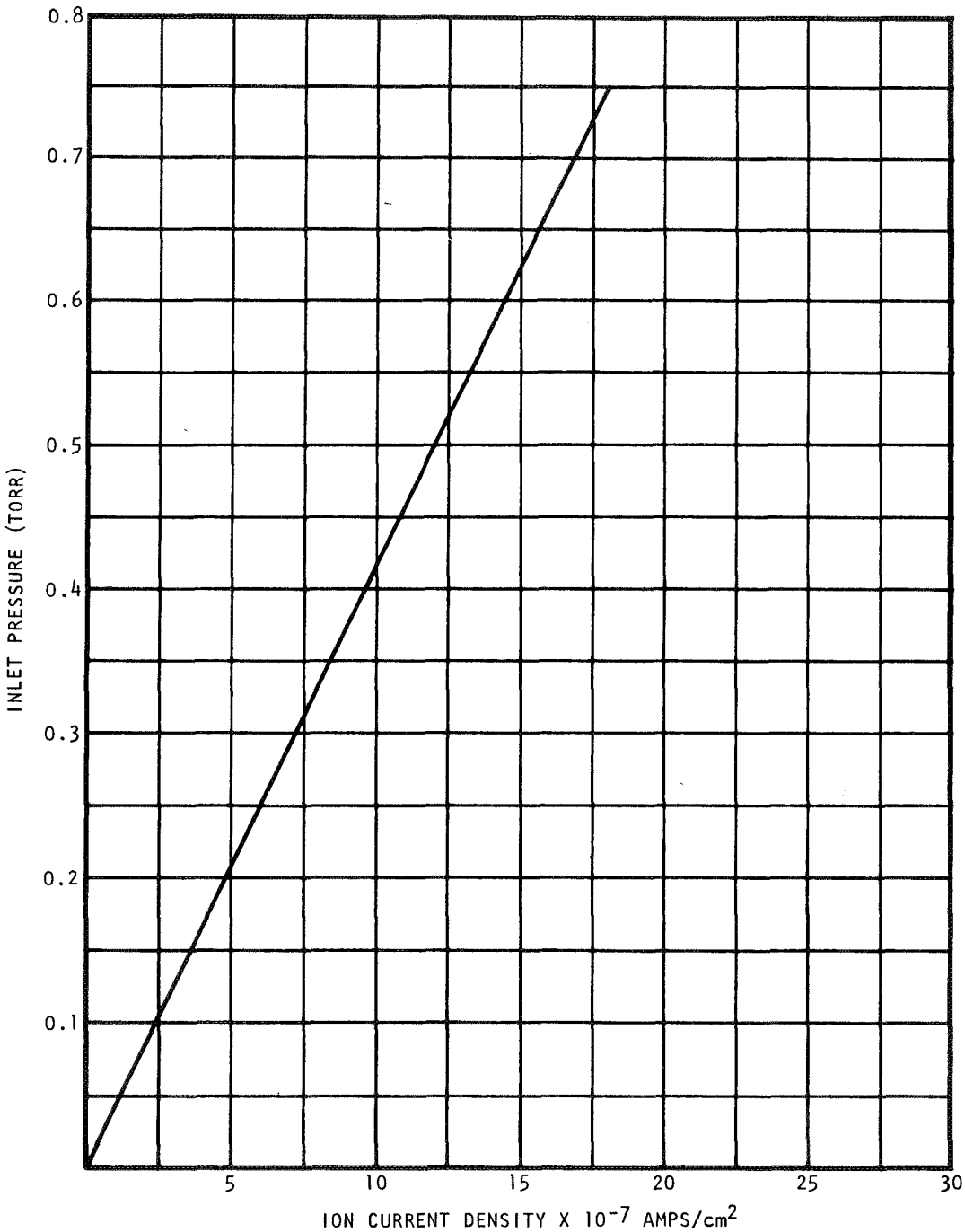

FIGURE 5.- Ion Current Density as a Function of Inlet Gas Pressure

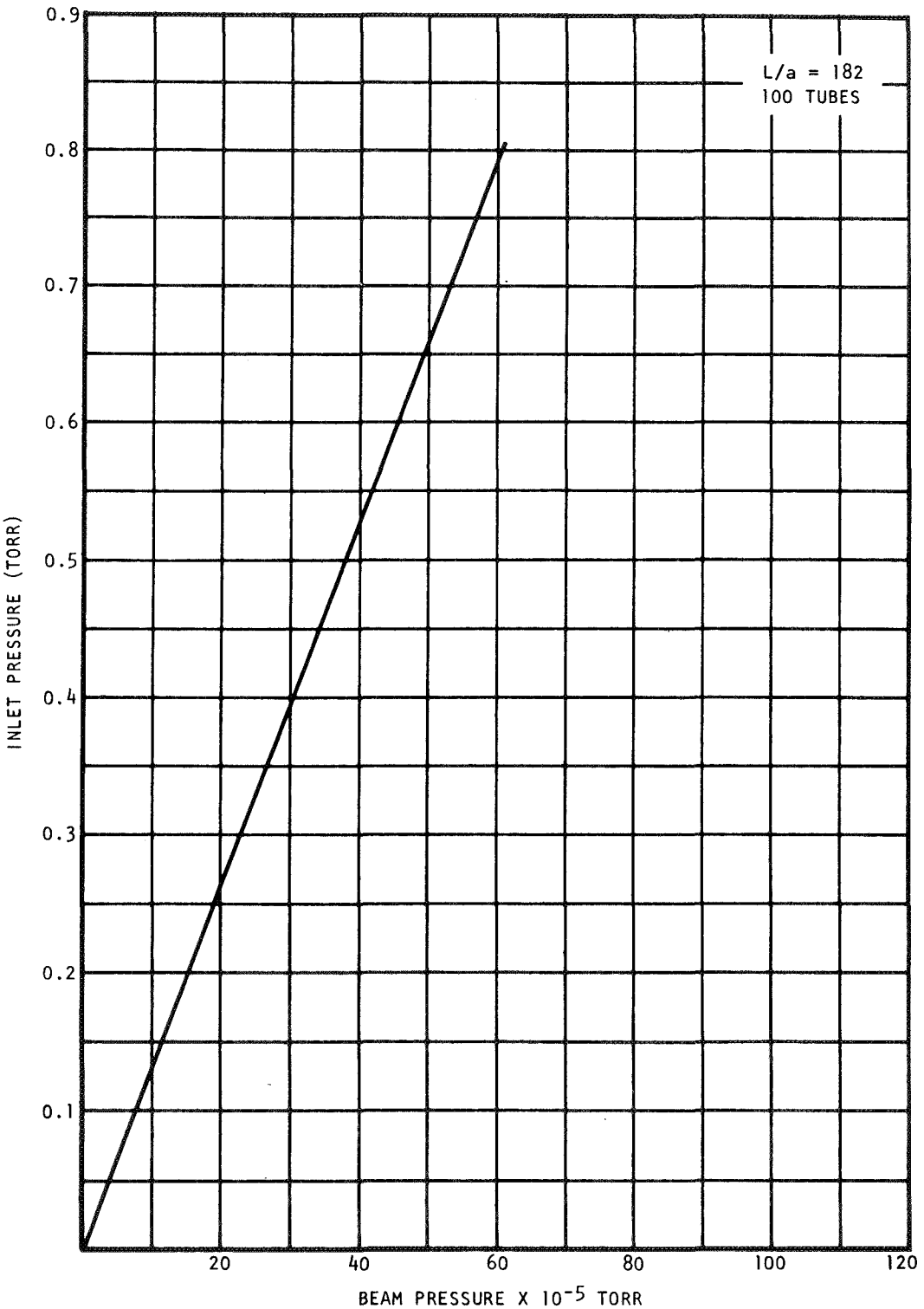

FIGURE 6.- Variation of Beam Pressure as a Function of Inlet Pressure

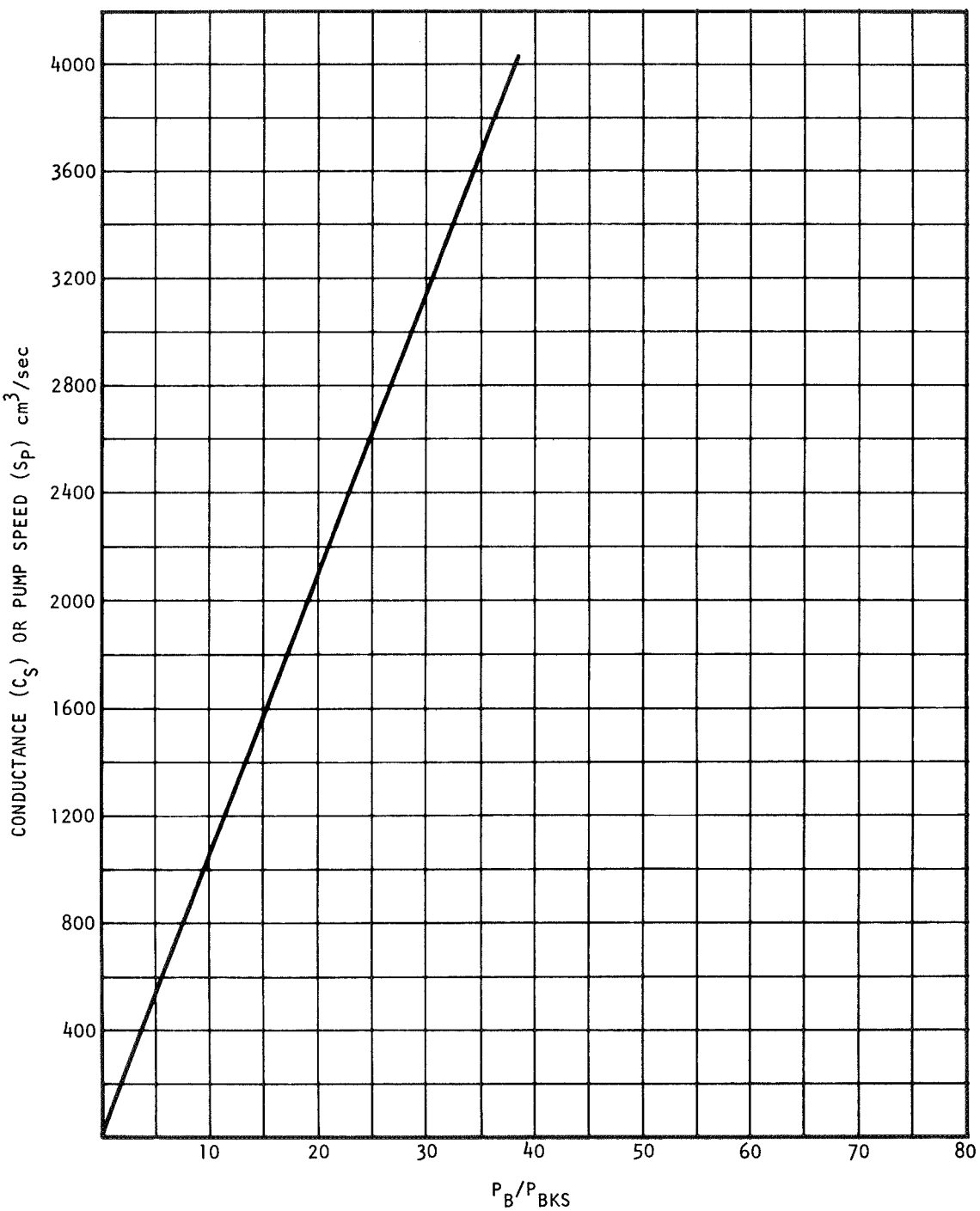

FIGURE 7.- Effect of Source Conductance (C_S) and Pump Speed (S_p) on the P_B/P_{BKGD} Ratio